8-2011

Aberrations Of A Putative Tumor Suppressor Gene Sel1L In Pancreatic Ductal Adenocarcinoma

Qian Liu

ABERRATIONS OF A PUTATIVE TUMOR SUPPRESSOR GENE *SEL1L* IN PANCREATIC DUCTAL ADENOCARCINOMA

By

Qian Liu, M.D.

APPROVED:

(Marsha L. Frazier, Ph.D., Supervisory Professor)

(Ann M. Killary, Ph.D.)

(Subrata Sen, Ph.D.)

(Christopher Amos, Ph.D.)

(Peng Huang, M.D., Ph.D.)

(Jan Bressler, Ph.D.)

APPROVED:

Dean, The University of Texas

Health Science Center at Houston

Graduate School of Biomedical Sciences

ABERRATIONS OF A PUTATIVE TUMOR SUPPRESSOR GENE *SEL1L* IN PANCREATIC DUCTAL ADENOCARCINOMA

A dissertation presented to the Faculty of

The University of Texas

Health Science Center at Houston

and

The University of Texas

M. D. Anderson Cancer Center

Graduate School of Biomedical Sciences

In partial fulfillment of the requirements for the

Degree of Doctor of Philosophy

By

Qian Liu, M.D.

Houston, Texas

August, 2011

ACKNOWLEDGMENTS

I would like to thank my advisor Dr. Marsha Frazier for giving me the opportunity to work in her esteemed laboratory and always being supportive. I sincerely appreciate all the things that she taught me in these years.

I would like to thank all my committee members: Drs. Ann Killary, Subrata Sen, Christopher Amos, Peng Huang and Jan Bressler for their guidance and valuable suggestions.

I would like to thank all the lab members who worked with me: Chongjuan Wei, Jane Chen, Elsie Wu, Jing Zhu, Matilde Olive, Mila Patenia, Haidee Chancoco, Imelda Campos, Veronica Gutierrez, Mala Pande, Xiaopei Wang, Joshua Amos, Joshua Rother, Luis Orta and Daniel Osterwisch for their help and support, as well as providing a family-like work environment.

I would like to thank Hongli Tang at the DNA Analysis Core Facility in UTMDACC for the technique support, and Drs. Nanyue Chen, Jin Wang and Seetharaman Balasenthil for their comments regarding this work.

I would like to thank my parents for their encouragement and selfless help. I would also like to thank my husband Zhibo and my two boys Eric and Gavin for the happiness they have brought to me.

Last, I would like to thank GSBS for giving me such a wonderful learning experience, and to gratefully acknowledge the following grant support: National Cancer Institute U01 Grant CA11130, Cancer Center Support Grant CA16672 and National Institute of Health R25 Educational Grant CA56452.

ABERRATIONS OF A PUTATIVE TUMOR SUPPRESSOR GENE *SEL1L* IN PANCREATIC DUCTAL ADENOCARCINOMA

Publication No._____

Qian Liu, M.D.

Supervisory Professor: Marsha L. Frazier, Ph.D.

ABSTRACT

Introduction: Pancreatic cancer is the fourth leading cause of cancer-related death among males and females in the United States. *Sel-1-like* (*SEL1L*) is a putative tumor suppressor gene that is downregulated in a significant proportion of human pancreatic ductal adenocarcinoma (PDAC). It was hypothesized that *SEL1L* expression could be down-modulated by somatic mutation, loss of heterozygosity (LOH), CpG island hypermethylation and/or aberrantly expressed microRNAs (miRNAs).

Material and methods: In 42 PDAC tumors, the *SEL1L* coding region was amplified using reverse transcription polymerase chain reaction (RT-PCR), and analyzed by agarose gel electrophoresis and sequenced to search for mutations. Using fluorescent fragment analysis, two intragenic microsatellites in the *SEL1L* gene region were examined to detect LOH in a total of 73 pairs of PDAC tumors and normal-appearing adjacent tissues. Bisulfite DNA sequencing was performed to determine the methylation status of the *SEL1L* promoter in 41 PDAC tumors and 6 PDAC cell lines. Using real-time quantitative PCR, the expression levels of *SEL1L* mRNA and 7 aberrantly upregulated miRNAs that potentially target *SEL1L* were assessed in 42 PDAC tumor and normal pairs. Statistical methods were applied to evaluate the

correlation between *SEL1L* mRNA and the miRNAs. Further the interaction was determined by functional analysis using a molecular biological approach.

Results: No mutations were detected in the *SEL1L* coding region. More than 50% of the samples displayed abnormally alternate or aberrant spliced transcripts of *SEL1L*. About 14.5% of the tumors displayed LOH at the CAR/CAL microsatellite locus and 10.7% at the RepIN20 microsatellite locus. However, the presence of LOH did not show significant association with *SEL1L* downregulation. No methylation was observed in the *SEL1L* promoter. Statistical analysis showed that *SEL1L* mRNA expression levels significantly and inversely correlated with the expression of hsa-mir-143, hsa-mir-155, and hsa-mir-223. Functional analysis indicated that hsa-mir-155 acted as a suppressor of *SEL1L* in PL18 and MDAPanc3 PDAC cell lines.

Discussion: Evidence from these studies suggested that *SEL1L* was possibly downregulated by aberrantly upregulated miRNAs in PDAC. Future studies should be directed towards developing a better understanding of the mechanisms for generation of aberrant *SEL1L* transcripts, and further analysis of miRNAs that may downregulate *SEL1L*.

TABLE OF CONTENTS

LIST OF FIGURES

LIST OF TABLES

BACKGROUND

1. Pancreatic cancer

The pancreas is an organ which has both endocrine and exocrine components. The endocrine component secretes hormones into the blood. Microscopically, the endocrine pancreas is made of cell clusters called islets of Langerhans which consist of five types of cells: alpha cells, beta cells, delta cells, PP cells and epsilon cells. Acinar cells of the exocrine pancreas produce and secret digestive enzymes and pancreatic juice (an alkaline fluid) into the small intestines through the exocrine ducts. Pancreatic cancer usually arises from the exocrine portion of pancreas [1].

In the United States, pancreatic cancer is the fourth leading cause of cancer-related death among males and females. “The American Cancer Society's most recent estimates for pancreatic cancer in the United States for 2010 are: about 43,140 new cases (21,370 men and 21,770 women), and about 36,800 deaths (18,770 men and 18,030 women). The lifetime risk for developing pancreatic cancer is about 1 in 71 (1.41%), which is about the same for both men and women.” Tobacco smoking, family history of pancreatic cancer, personal history of pancreatitis, diabetes and obesity are all commonly recognized risk factors for this type of cancer [2]. Since the symptoms of pancreatic cancer are non-specific and varied, usually by the time it is diagnosed local or distant metastasis has already occurred. Prognosis for this disease is very poor with a median survival time of less than 6 months for all patients diagnosed with this disease, and the overall 5-year survival is only 6% [3]. The most common

form of pancreatic cancer is pancreatic ductal adenocarcinoma (PDAC), which accounts for >75% of all pancreatic tumors [4].

Histologically, PDAC is an invasive malignant epithelial neoplasm with no predominant component of any of the other carcinoma types. The appearance and arrangement of the PDAC cells present a duct-like structure instead of the predominant acinar cell structure seen in normal pancreas. “The degree of gland (duct) formation can vary from well-formed glands, to partially formed glands, to focal intracellular mucin production by poorly oriented cells infiltrating singly, to solid sheets of neoplastic cells.” [5] Although PDAC has a ductal morphology, there is no formal proof demonstrating that it originates from the ductal compartment.

Acinar-to-ductal metaplasia has been implicated in the generation of pancreatic cancer precursor lesions known as pancreatic intraepithelial neoplasia (PanIN) [6-8]. Metaplasia is defined as a predominant cell type in a tissue being replaced by another cell type. There is evidence for at least two pathways for development of acinar-to-ductal metaplasia. In the first, abnormal acinar cells transdifferentiate to ductal cells and then proliferate. In the second, ductal cells proliferate and the abnormal acinar cells undergo apoptosis.

Animal models have been used to study the process of acinar-to-ductal metaplasia. Guerra et al. selectively expressed K-*RAS*^{G12V} in mice embryonic cells of the acinar/centroacinar lineage and observed the formation of PanIN lesions and invasive PDAC [9]. Similarly, Habbe et al. reported that knockin of the K-*RAS*^{G12D} allele in mature acinar cells of adult mice resulted in spontaneous induction of murine PanIN lesions of all histological grades [10]. By performing murine pancreatic

epithelial explants, Dr. Leach's group showed spontaneous acinar-to-ductal metaplasia in response to EGFR signaling. The transdifferentiated cells simultaneously express both acinar and ductal markers [11].

In summary, all these models provided evidence that the genetic signature of pancreatic cancer involves genetic alterations in PanIN lesions that may induce acinar-to-ductal cell transdifferentiation and further development into PDAC.

2. Genetic alterations in the pathogenesis of PDAC

Many allelic alterations have been seen in PDAC, including losses of 1p, 9p, 12q, 17p, 18q and gain of 20q [12-18]. Several of these have been demonstrated to be involved in the progression of PDAC. The early genetic changes include the aberrant activation of the epidermal growth factor receptor (EGFR), erbB2 (HER2), v-Ki-ras2 Kirsten rat sarcoma viral oncogene homolog (K-Ras), and the inactivation of Cyclin-dependent kinase inhibitor 2A (CDKN2A/p16-INK4A) and alternative reading frames of the INK4A (ARF) tumor suppressor proteins [19-21]. Loss of two tumor suppressors, TP53 (p53) and BRCA2, frequently occur in the progression of the pancreatic intraepithelial neoplastic (PanIN) lesions. Loss of SMAD4/DPC4 function occurs at later stages [19, 20]. Overexpression of various components of Hedgehog (Hh) signaling including Shh and Ihh also have been seen in PanIN lesions as well as invasive PDAC [22-24]. An oncogenic serine/threonine kinase, AURKA, also showed overexpression in PDAC [25, 26]. The 9p21 region harbors the *p16-INK4A* gene; the 17q13 region harbors the *p53* gene; the *SMAD4* gene is located on chromosome 18q21 and *AURKA* maps to chromosome 20q13. Therefore, allelic loss or gain may explain

some of the gene expression alterations. Many signaling pathways can be affected by the above genetic abnormalities, such as the EGFR signaling pathway, the Ras signaling pathway, the transforming growth factor-beta (TGFβ) signaling pathway, as well as the Hedgehog (Hh) pathway and the Wnt–β-catenin cascades [27].

However, all the above genetic alterations have also been observed in many other kinds of cancers, so unfortunately none of these serve as PDAC tumor specific biomarkers.

3. *SEL1L* gene and PDAC

Seven genes were identified in Dr. Killary's laboratory, which were found to be differentially expressed in PDAC across three platforms. Products of these genes could serve as candidate biomarkers for PDAC [28]. One of the genes, *SEL1L,* has been shown to be abundantly expressed specifically in pancreatic tissues from healthy adult humans [29, 30]. Biunno et al. reported that *SEL1L* messenger RNA (mRNA) was not detected in 17% of PDAC tumors by reverse-transcription polymerase chain reaction (RT-PCR) [29]. Downmodulation or absence of SEL1L protein has been seen in 36% of human PDAC cases by immunohistochemistry. Immunohistochemical staining revealed that SEL1L protein is highly expressed in normal pancreatic acinar and islet cells, whereas it is not expressed in normal ductal cells [31]. Therefore, a question was raised that whether SEL1L downregulation was caused by the difference in cell types between normal pancreas and PDAC tumors. To answer this question, understanding the cellular origin of PDAC is a key. Acinar to ductal

transdifferentiation in some model systems suggests that acinar cells may be the cell of origin, and this may explain why SEL1L is expressed in some PDACs.

SEL1L has been shown to modulate the expression of certain cancer-related proteins. In *C. elegans*, sel-1 has been identified as a negative regulator of the lin-12/Notch family oncoproteins, lin-12 and glp-1. This is likely through its function in protein degradation [32, 33]. Overexpression of *SEL1L* in stably transfected PDAC cells and in nude mice caused a decrease in the aggressive behavior of the tumor cells, suggesting that *SEL1L* plays a tumor-suppressive role in the progression of PDAC [31]. Overexpression of *SEL1L* in PDAC cells also showed a significant increase in the expression level of the tumor suppressors Smad4, activin A, TIMP1, TIMP2, and PTEN, suggesting an interaction of SEL1L with the TGFβ and PTEN signaling pathways [31, 34].

4. *SEL1L* gene and SEL1L protein

The *homo sapiens SEL1L* gene is located on chromosome 14q24.3-q31 with a length of 60967 base pairs (bp). It consists of 21 exons and the corresponding full length mRNA contains 6593 bp and the coding region is 2385 bp long. According to the gene annotations in the AceView database, National Center for Biotechnology Information (NCBI), the *SEL1L* gene produces 10 different transcripts that potentially encode 8 different isoforms [35].

At the N terminus of the SEL1L protein, there is an XXRR-like ER (endoplasmic reticulum) membrane retention signal, and a proline, glutamic acid, serine, and threonine peptide (PEST) sequence which is known to target proteins for

rapid degradation. The SEL1L protein also contains a fibronectin type II domain which is a collagen-binding domain, three SEL-1-like sequence clusters in tandem which are predicted to function in protein-protein interaction, one highly conserved Hrd3-like motif which also has predicted function in protein binding, one transmembrane domain, and one proline-rich tail which may bring proteins together. Hrd3 is a protein of the ER membrane that plays a central role in ER associated protein degradation (ERAD). The Hrd3 protein motif is shared with several other proteins [36, 37]. From the protein structure, SEL1L is predicted to be an ER membrane protein with functions of protein-protein interaction and protein degradation. It has been reported that the region of SEL1L spanning amino acids 659 to 794 containing the Hrd3-like motif, the transmembrane domain and the proline-rich tail is required for tumor growth inhibition [38].

5. SEL1L and UPR/ERAD pathway

The human homolog of *SEL1L* has been recognized as a component of the "unfolded protein response/endoplasmic reticulum associated protein degradation (UPR/ERAD) pathway" [36, 39, 40]. The pancreas is an organ that produces many important proteins, such as insulin, glucagon and digestive enzymes [1]. Endoplasmic reticulum is an organelle found in all eukaryotic cells which functions in protein translation, folding, export and secretion [41]. Therefore, the ER is a critical organelle for synthesis and secretion of the many proteins made in the pancreas.

Certain pharmacological or physiological conditions such as hypoxia, redox or glucose starvation, may lead to an accumulation of unfolded or misfolded proteins in

the lumen of the ER and cause ER stress. The UPR/ERAD pathway is triggered in response to the stress and induces the activation of several additional signaling pathways to promote long-term stress adaptation or apoptotic cell death [42].

Figure 1 shows a simplified version of the URP/ERAD pathway. The primary function of this pathway is to maintain ER homeostasis and produce cell survival after stress. When this pathway is activated, the ER chaperone glucose-regulated protein 78 (GRP78), the serine/threonine kinase Akt, the nuclear factor NF-κB, and the anti-apoptosis factor Bcl-2/xL are induced [43-49]. Consequently, cell proliferation and angiogenesis are promoted. Simultaneously, the E3 ubiquitin-protein ligase HMG-CoA reductase degradation protein 1 (HRD1) and SEL1L are also induced by the ER stress. SEL1L interacts with and stabilizes HRD1, and also recognizes misfolded proteins and transfers them into the cytosol for degradation [37-39]. On the other hand, when the accumulated unfolded proteins exceed a threshold above which the ER stress can no longer be controlled, the cell becomes committed to apoptosis through another part of the UPR pathway. Gadd153/CHOP is the dominant ER chaperone that is induced [50]. Caspase-4, a caspase responding only to ER stress and not to other signals, is activated [51]. When SEL1L expression was knocked down in mouse pancreatic β-cells, a decrease in cell growth was observed. This may be through activation of the apoptosis pathway described above [52].

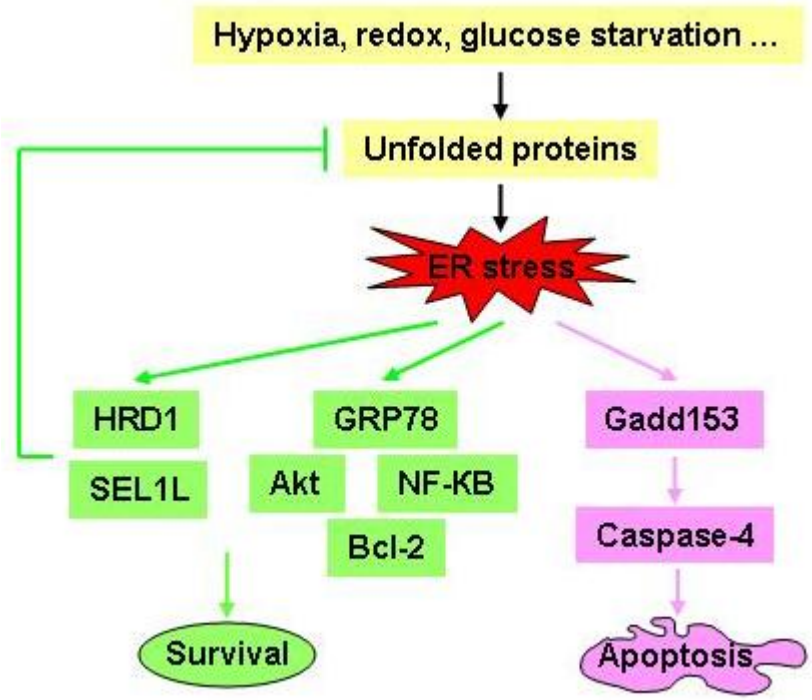

Figure 1. Unfolded protein response/endoplasmic reticulum associated protein degradation (UPR/ERAD) pathway. Green: survival pathway; pink: apoptosis pathway.

6. The goals of this study

So far neither mutations nor genomic alterations have been reported for *SEL1L* which is a putative tumor suppressor in PDAC. The goals of this study were to investigate the molecular mechanisms of SEL1L downregulation, and to better understand the role of SEL1L in the pathogenesis of PDAC. I hypothesized that SEL1L expression could be down-modulated by somatic mutation, loss of heterozygosity (LOH), CpG island hypermethylation and/or aberrantly expressed microRNAs (miRNAs). Results from this study provide a better understanding of the abnormalities of the *SEL1L* gene in PDAC, which may lead to the discovery of PDAC tumor specific biomarkers or the development of new prevention and treatment strategies for this dismal disease.

Chapter 1

SEL1L Gene Mutation Study

1.1 Introduction

Due to genetic instability, cancer cells often carry somatic mutations in either tumor suppressor genes or oncogenes. Somatic mutations occurring at the splice sites or exonic splicing enhancers may cause aberrant transcription, and may lead to the translation of aberrant proteins. Mutations occurring at the coding region of a gene may also produce aberrant proteins, which may influence the function of the gene. Mutations in some predominant cancer-related genes have been frequently reported in PDAC tumors. For example, *Kras* mutations are some of the earliest events in the tumorigenesis of PDAC, which have been detected in 90% of PDACs with most of the mutations occurring at codon 12, 13, and 61; loss of the *p53* gene often occurs later in the development of pancreatic neoplasia, generally by missense alterations of the DNA-binding domain in more than 50% of PDACs [18-20].

So far, only one study of *SEL1L* gene alterations in PDAC has been conducted. In this study Southern blotting was performed on 17 neoplastic cases, but no gross genomic alterations were observed [28]. The Southern blotting method uses probe hybridization to identify a restriction fragment of a gene. However, in this report the authors did not give the exact region that they examined, and apparently they did not examine the whole gene region of *SEL1L*. Their results might not give an accurate conclusion, and it is still important to determine if somatic mutations are present in the *SEL1L* gene. Therefore, I chose to examine *SEL1L* for mutation in PDAC samples.

1.2 Materials and Methods

Materials

PDAC tumors and the matched normal-appearing adjacent pancreatic tissue specimens were collected from surgical resections performed at The University of Texas M. D. Anderson Cancer Center (UTMDACC) before patients were treated with chemotherapy or radiotherapy. The identification of normal adjacent tissue was based on microscopical observations from the pathologist analyzing the tissue. All the tissues were stored in -80ºC freezers prior to RNA/DNA extraction. A total of 42 tumor/normal pairs were examined in this study. A quality check of integrity with the 2100 Bioanalyzer (Agilent Technologies, Santa Clara, CA) indicated that the RNA samples did not display degradation.

Extraction of RNA and DNA

Total RNA was extracted using the miRNeasy Mini Kit according to the manufacturer's instructions (Qiagen, Valencia, CA). DNA was extracted from the inter-phase and phenol phase after RNA isolation. The isolation procedures followed the TRIzol Reagent protocol (Invitrogen, Carlsbad, CA). DNA and RNA concentrations were measured with a NanoDrop spectrophotometer (Thermo Scientific, Wilmington, DE).

Reverse transcription polymerase chain reaction (RT-PCR) and sequencing

The High Capacity cDNA Reverse Transcription Kits (Applied Biosystems, Foster City, CA) were used for complementary DNA (cDNA) synthesis. The conversion to cDNA started from 1ug of total RNA in a single 20μL reaction using random primers. To amplify the cDNA with high fidelity, three sets of primers were used for the entire coding region of SEL1L, and the RT-PCR products overlapped one another by about 100 bp.

The SELmRNA-1 primer set generates a product of 934 bp which extends from *SEL1L* exon 1 to 7. SELmRNA-2 generates a 972 bp product which is from exon 6 to 17. SELmRNA-3 amplifies exon 16 to 21 and the product size is 987 bp. Sequences and locations of the primers were shown in Figure 2. The reactions were carried out in a final volume of 30 uL of a mixture containing 2μL of cDNA, 10 pmol of each primer, deoxynucleotide triphosphates (dNTP, each at 0.25 mM), KCl (50 mM), $MgCl_2$ (1.5 mM), Tris-HCl (10 mM, pH 8.3), and 1 unit of AmpliTaq Gold DNA polymerase (Applied Biosystems). The same thermal cycling conditions were applied to all 3 reactions: denaturation at 95°C for 5 minutes for 1 cycle, followed by 40 cycles at 95°C for 45 seconds, 56°C for 45 seconds, 72°C for 45 seconds, and then an extension of 72°C for 7 minutes. A 5 uL aliquot of the RT-PCR products was run through 1% agarose gel (Phenix Research Product, Candler, NC) using 100 bp DNA ladder as a molecular weight marker (Invitrogen). The remainder of the products were purified with QIAquick PCR Purification Kit (Qiagen), and then sequenced in the DNA Analysis Facility at UTMDACC using ABI PRISM 3730 DNA sequencers (Applied Biosystems).

A.

Primer Name	Forward	Reverse
SELmRNA-1	5'-agg aag gag act aga gca gga ag-3'	5'-ctt gaa tta aca cca agt cca gag-3'
SELmRNA-2	5'-tta ttt ggt gat tac ttg cca cag-3'	5'-gcc tcg ttc aca tac att ctt aaa-3'
SELmRNA-3	5'-ggc att gga gtc aag aga gat tat-3'	5'-act gat cca agg tcc taa atc aaa-3'

B.

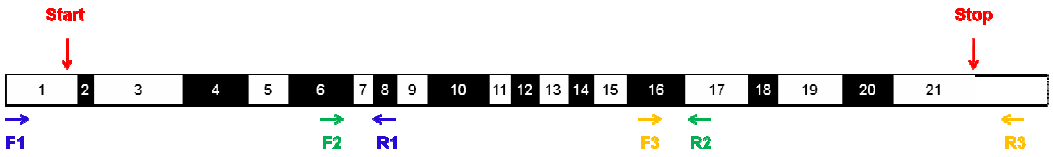

Figure 2. Sequences and locations of the primers for *SEL1L* coding region mutation study. The rectangular boxes in figure B represent the exons in SEL1L cDNA. Translation start site and stop site were indicated. F1 and R1 indicate the locations of forward and reverse primers of SELmRNA-1; F2 and R2 are SELmRNA-2; F3 and R3 are SELmRNA-3.

1.3 Results

Altered SEL1L *transcripts in PDAC tumors and paired normal-appearing adjacent tissues*

When reverse-transcribed mRNAs were amplified using the SELmRNA-1 primer sets, agarose gel electrophoresis revealed that in addition to the predicted RT-PCR products, some weaker products with smaller sizes were present. These smaller products were observed in both PDAC tumor tissues and normal-appearing adjacent tissues. This phenomenon was not observed when the cDNAs were amplified using the SELmRNA-2 and SELmRNA-3 primer sets. The representative results from 7 tumor/normal pairs are shown in Figure 3. When the RT-PCR was repeated using the SELmRNA-1 primers, although additional products were observed again, different patterns of products were present. From the results of two independent RT-PCR amplifications, additional products were identified in more than half of the samples.

Because most of the unexpected small products had much lower intensities, nucleotide sequence analysis usually displayed only the sequence of the predominating normal products. However, in a few of the samples one smaller product showed competitive intensity compared to the expected product. Sequencing chromatograms of these samples showed identifiable double peaks, so that the sequence of both products could be analyzed. Figure 4 shows such a chromatogram displaying the out of phased sequence indicating deletions.

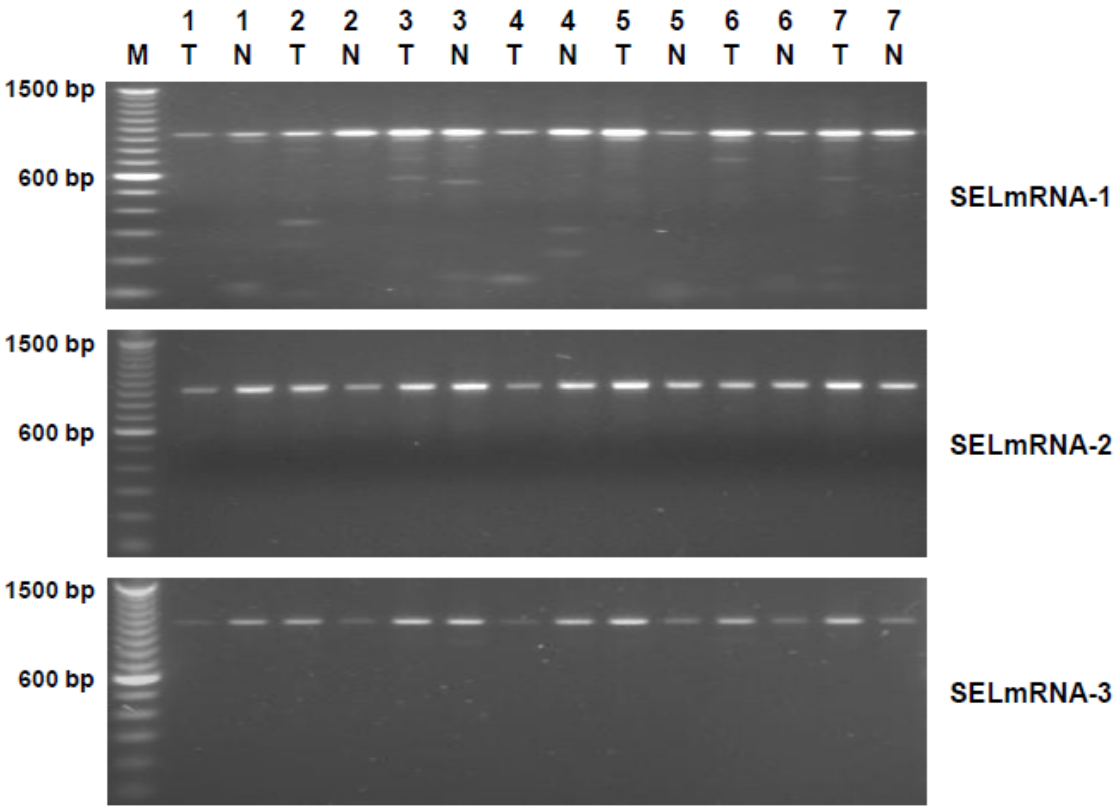

Figure 3. Agarose gel electrophoresis of representative RT-PCR products of *SEL1L* coding region. M, marker. T, PDAC tumor. N, normal-appearing pancreatic tissue. Specimens from the same patient have the same number. Names of primer sets are noted at the right.

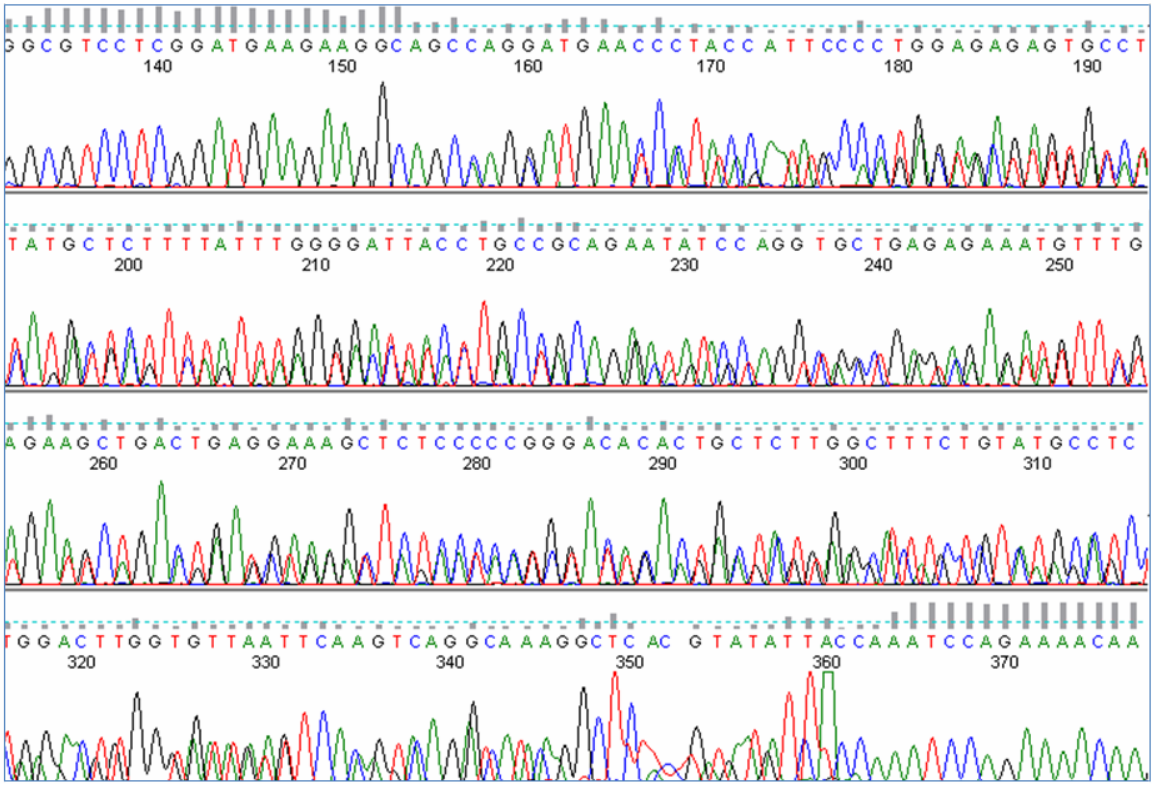

Figure 4. A sequencing chromatogram displays double peaks. The RT-PCR products of a PDAC tumor sample were produced using SELmRNA-1 primers. The out-of-phase sequence starts at position 157 and extends to position 360, indicating the existence of two products in this sample.

Figure 5 shows SEL1L mRNA RT-PCR products from 5 representative samples. In Figure 5A, using agarose gel electrophoresis, multiple different products with competitive intensities can be identified in the 5 samples. Figure 5B schematically presents a diagram of the sequencing results of the full-length (FL) normal product and the small aberrant products. The 497bp fragment in sample 1 skipped exons 4, 5, and 6 and potentially encodes a truncated protein of 125 amino acids (aa). In sample 2, exon 3 was skipped and a stop codon was introduced in exon 4 so that a protein of 37 aa could be generated. The sequence of the 871-bp fragment in sample 3 showed that 63 bp from the beginning of exon 4 was spliced through a novel AG splice acceptor site. The predicted amino acid sequence is in-frame with 21 aa deleted. In the 293-bp fragment of sample 4, a non-conserved donor site in exon 2 was joined to a non-conserved acceptor site in exon 6. Both the donor and acceptor contain a 7-base sequence of AGGCAGC. The frameshift of this fragment would produce a 32-aa truncated protein. Similar aberrant splicing happened in sample 5 as was seen in sample 4. The splicing donor site in sample 5 was the same as in sample 4, but the acceptor site was at a different location in exon 6. A 46-aa protein would be encoded.

These sequencing results indicated that the smaller products arose as a result of mis-splicing of the *SEL1L* pre-mRNA, but none of these products are included in the NCBI transcription annotation database (AceView). This database is supposed to provide a comprehensive and non-redundant sequence representation of all public mRNA sequences [33]. Commonly, mis-splicing occurring at intron-exon boundaries is referred to as alternate splicing; and splicing occurring at cryptic splice sites (within

intron or exon) is referred to as aberrant splicing. Here, samples 1, 2, and 3 showed alternate splicing, and samples 4 and 5 showed aberrant splicing.

Mis-splicing could be caused by mutations at the splicing sites. Therefore, of the 5 samples in Figure 5, polymerase chain reaction (PCR) products of the genomic sequences flanking the intron-exon boundaries and the non-conserved splicing sites were generated. No mutations were detected (data not shown here), indicating that the alteration of *SEL1L* splicing was not caused by genomic mutations.

Mutation is not detected in the SEL1L *coding region*

The sequence of the whole *SEL1L* coding region was determined for cDNA generated from 42 PDAC tumor samples and compared to the *SEL1L* coding sequence reported in Genbank using the BLAST computer algorithm [53], but no mutations were detected in any of them. Several single nucleotide polymorphisms (SNPs) were identified in the sequences that have been listed in the NCBI dbSNP database, including rs11499034 located in exon 4 in 1 sample, rs11851475 in exon 17 in 1 sample, and rs1051193 in exon 20 in 2 samples. The frequencies of these SNPs were close to the reported frequencies in the NCBI database in the normal population of Caucasians, indicating that these SNPs are normally present.

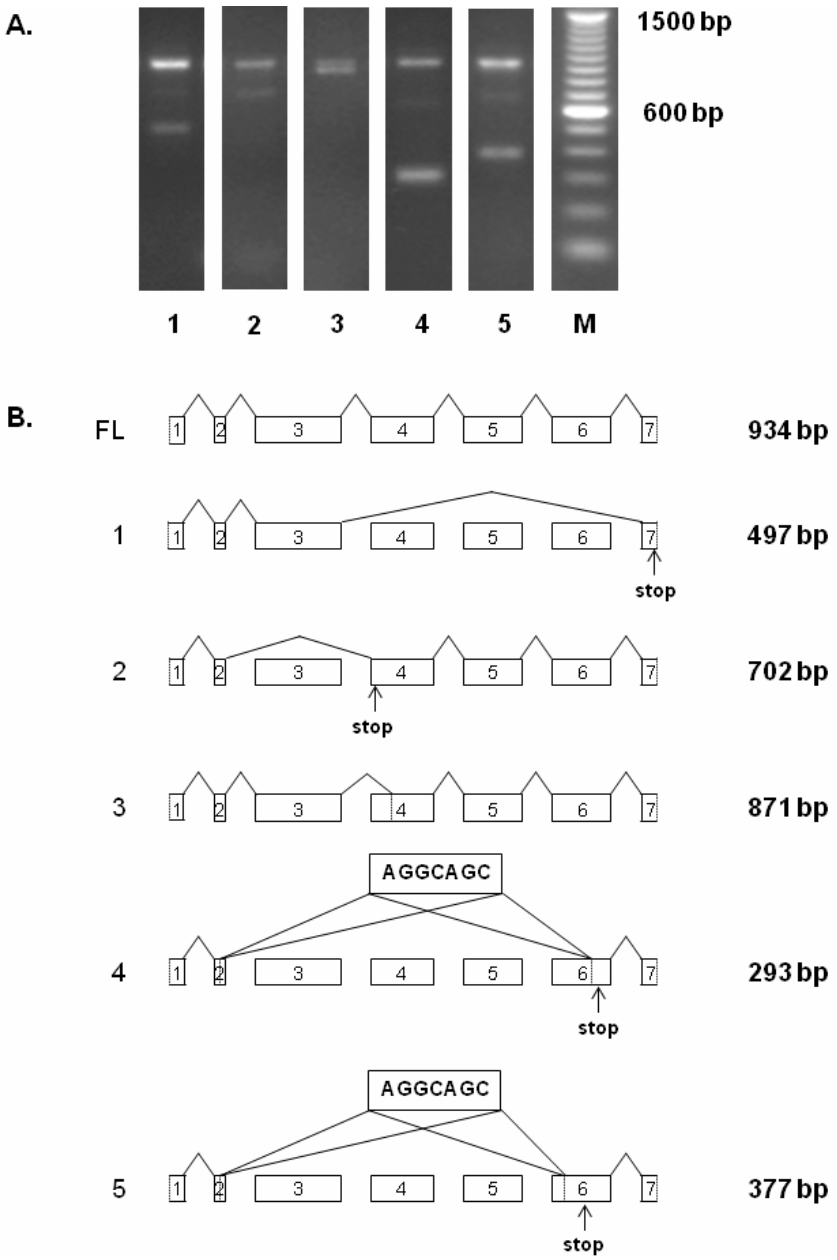

Figure 5. Alteration of SELmRNA-1 RT-PCR products in 5 PDAC tumors.

A. Agarose gel electrophoresis. M, marker. **B.** Schematic diagram of the smaller products in relation to the full-length fragment. FL, full-length (expected product). A broken line in an exon indicates an incomplete exon. Each rectangular box represents one exon. Arrows indicate the locations of stop codon for protein translation. RT-PCR product sizes are noted at the right.

1.4 Discussion

In this study, I investigated whether genetic mutations exist in the pancreas-specific putative tumor suppressor gene *SEL1L* in PDAC cases, and whether mutations are the cause of *SEL1L* downregulation. By amplifying and sequencing the coding region of *SEL1L* in 42 pairs of PDAC tumors and normal adjacent tissues, no mutations were detected; interestingly, however, unexpected altered splice forms of SEL1L pre-mRNA were observed.

Sequencing results revealed that these RT-PCR products were true *SEL1L* transcripts that were not generated from PCR artifacts or wrong priming. The unexpected splicing products that were observed were different from the normal *SEL1L* alternate transcripts that are annotated in the NCBI database. These unexpected *SEL1L* RT-PCR products had weak intensities on agarose gels, and the exact patterns were not reproducible. This lack of reproducibility is likely due to a low abundance of any given aberrant splice product.

The formations of the alternate/aberrant splice products shown in Figure 5 suggest that the splicing alterations of *SEL1L* most likely occur between exon 2 to exon 6. The protein sequence corresponding to this region involves a PEST sequence, a Fibronectin Type II (FNII) domain, and a SEL-1-like repeat. The predicted truncated SEL1L proteins missing these specific domains would lose their function in protein modulation. It is also possible that the dysfunctional proteins interrupt the tumor-suppressor function of normal SEL1L protein through a competition for target protein binding.

The same mis-splicing phenomena have been previously reported in other tumor suppressor genes in various cancers, such as tumor susceptibility gene 101 (*TSG101*) in breast and lung cancer [54, 55], Mdm2 p53 binding protein homolog (*MDM2)* in ovarian, bladder, and breast cancer [56-58], and fragile histidine triad gene (*FHIT*) in breast, head and neck, and lung cancers [59-61]. In PDACs, abnormal transcripts have been observed in cholecystokinin-B/gastrin receptor (*CCKBR*) [62] and Mucin type 4 (*MUC4*) [63].

Similar to what has been seen for the *TSG101*, *MDM2* and *FHIT* genes, abnormal products in normal-appearing tissues adjacent to the tumor were observed. One reason could be due to the fact that the PDA tumor/normal paired tissue samples were obtained without using precise microdissection techniques. Therefore, the normal-appearing samples could be contaminated with some tumor cells, or there may have been a field effect in the normal-appearing tissue that was in close proximity to the tumor, or there could have been micrometastasis to normal-appearing pancreatic tissue.

As has been reported for those genes mentioned above, I determined that the aberrant *SEL1L* splicing was also not caused by genomic DNA sequence alterations. Aberrant expression of splicing factors may be the mechanism for the mis-splicing. For instance, a core splice regulatory protein serine-arginine protein kinase 1 (SRPK1) has shown up-regulation in pancreatic carcinomas [64]. Aberrant splicing factors may cause binding to (or failure to bind to) splice enhancers located in the *SEL1L* gene regions. This could explain why mis-spliced products were observed from the RT-PCR using SELmRNA-1 primers but not SELmRNA-2 and -3 primers. The increase

in aberrant splicing could also be caused by the changes of environmental factors, such as elevated temperature and low pH that are frequent occurrences in tumor tissues. A study of the tumor suppressor genes neurofibromatosis type 1 (*NF-1*), neurofibromatosis type 2 (*NF-2*), and tuberous sclerosis 2 (*TSC-2*) conducted by Dr. Kaufmann et al. suggested that the environmental alterations might change the structures at the splice donor site and disturbed splicing [65].

Elela and colleagues [66, 67] used high-throughput RT-PCR and deep sequencing to analyze the alternative splicing profiles of cancer-associated genes in normal and tumor tissues for both ovarian and breast cancer. They found that certain alternative splicing events significantly differed in the tumors relative to normal tissues. However, the method that was used in this study could not provide a full view of the alternative splicing events in the samples analyzed. Lukas et al. reported that the presence of the aberrant splicing products of *MDM2* in breast cancer specimens was correlated with a shorter overall patient survival [58]. Their results suggest that aberrant splicing in a tumor suppressor gene could be of clinical importance for cancer patients.

To determine whether there are tumor-specific *SEL1L* transcripts in PDAC, further tests with microdissected tissues and deep sequencing are necessary. Also because of the limitation of the material and methods used in this study, I was unable to determine whether mis-splicing was associated with the altered expression of *SEL1L* in PDAC.

Chapter 2

Loss of Heterozygosity in the *SEL1L* Gene

2.1 Introduction

Loss of heterozygosity (LOH) is defined as the loss of one allele in a tumor at a constitutionally heterozygous locus, and indicates loss of detection of one of the two alleles at that locus. LOH can arise via several pathways, including deletion, gene conversion, mitotic recombination, chromosome loss and amplification of one allele [68]. When there is only one functional allele left on the other chromosome, the product of a gene with LOH may be reduced, and it may not be expressed at levels sufficient to permit the cell to function normally. LOH is a common occurrence in cancer. In pancreatic adenocarcinomas, such allelic loss has been frequently observed at chromosome 9p which contains the *p16* gene, 17p which contains the *p53* gene, and 18q which harbors *SMAD4* [11, 69].

Microsatellites are good markers for LOH studies. Microsatellites are short tandem repeats of DNA that are distributed throughout the genome. The number of repeats often varies between two alleles, providing a high frequency of allelic heterozygosity. Two polymorphic intragenic microsatellites containing cytosine-adenine (CA) repeats in the *SEL1L* gene in the Italian population have previously been described by Chiaramonte et al. CAR/CAL microsatellite is located in *SEL1L* intron2 and was reported with a heterozygosity frequency of 0.68; RepIN20 microsatellite is located in intron20 with a heterozygosity frequency of 0.85 [70]. No other microsatellites have been found in the *SEL1L* gene locus.

In this chapter, using these 2 microsatellite markers, I aimed to determine whether LOH is observed at the *SEL1L* gene locus in PDAC, and whether LOH correlates with the downregualtion of *SEL1L*.

2.2 Materials and Methods

Materials

PDAC tumors and the matched normal-appearing adjacent pancreatic tissue specimens were collected as described in Chapter 1. A total of 73 pairs of DNA samples were tested in this study.

Real-time quantitative PCR (qPCR)

The expression levels of *SEL1L* mRNA were examined in the DNA Analysis Facility at UTMDACC. The TaqMan Gene Expression Assay kit targeting *SEL1L* (Applied Biosystems, Foster City, CA) were used for the assays. The assays were run using the 7900HT Fast Real-Time PCR System (Applied Biosystems). RNA from the matched normal-appearing adjacent tissue was used as a calibrator for the tumor. *SEL1L* mRNA expression was normalized to that of glyceraldehyde-3-phosphate dehydrogenase (GAPDH). All of the assays were run in duplicate. The relative quantities (RQs) of mRNA or miRNA expression in the tumors were calculated as described by Livak and Schmittgen [71]. A gene was considered to be downregulated if $RQ \leq 0.5$ so that the gene expression in the tumor was less than half that in the normal-appearing adjacent tissue. A gene was considered to be upregulated if $RQ \geq 2$, which means that the gene expression in the tumor was more than twice that in the normal-appearing adjacent tissue.

Fluorescent fragment analysis

This technique involves using fluorescent primers during amplification to label PCR products as described by Canzian et al [72]. Two kinds of fluorescent dyes HEX and FAM were used for labeling. Two sets of primers were designed for each of the microsatellite regions. The PCR amplifications were all carried out in a final volume of 30 μL of a mixture containing 10 ng of DNA, 10 pmol of each primer, deoxynucleotide triphosphates (dNTP) each at 0.25 mM, KCl (50 mM), $MgCl_2$ (1.5 mM), Tris-HCl (10 mM, pH 8.3), and 1 unit of AmpliTaq Gold DNA Polymerase (Applied Biosystems, Foster City, CA).

For the intron 2 microsatellite, the primers were as follows: CAR/CAL-1 (forward 5′-HEX-AAA ATT ACT GAC CTA CAA GAG GG-3′ and reverse 5′-TGG GCT TGG TTA GTA CTT GG-3′). The reaction was started at 95°C for 5 minutes, followed by 40 cycles (95°C for 45 seconds, 55°C for 45 seconds, and 72°C for 45 seconds) and then an extension of 72°C for 7 minutes. For another set of primers CAR/CAL-2 (forward 5′-FAM-AAA AGG ACA GAA AAA GAC AGA TGG-3′ and reverse 5′-GGG AGA GCT CAA TCA ACC AA-3′), the same PCR protocol was applied except that the annealing temperature was 58.5°C. For the intron 20 region, the primers were: REPIN20-1 (forward 5′-HEX-CGT ATT GGA TTA CTG GTG GAA AG-3′ and reverse 5′-GGC AAG GAA CTG GGA AAG TTA C-3′) with an annealing temperature of 58.5°C, and REPIN20-2 (forward 5′-FAM-GCC CCA GTG TTG TTT TGT TT-3′ and reverse 5′-AGG CAA GGA ACT GGG AAA GT-3′) with an annealing temperature of 60°C.

Using a 3730 DNA Analyzer (Applied Biosystems), the PCR products were separated by capillary electrophoresis and analyzed in the DNA Analysis Facility at UTMDACC. Fluorescently labeled fragments were detected by the machine and the lengths of the fragments and fluorescent signal strengths were determined by analysis software. In the case of heterozygotes, the fluorescent signal strength of the PCR products from constituent alleles between tumor and its paired normal tissue was compared. A ratio was calculated as follows: (tumor peak 1 / tumor peak 2) / (normal peak 1 / normal peak 2). The average ratio from both primer sets was counted as the final result. A ratio greater than 1.500 (3/2) or less than 0.667 (2/3) was considered as positive evidence for the presence of LOH in the tumor. For example, in Figure 6B, the ratio was calculated as: (16273 / 5684) / (12073 / 9278), which is 2.127 and indicates that LOH displays in this tumor sample.

2.3 Results

LOH is detectable in a small proportion of the PDAC tumors

Figure 6 shows representative results of the fluorescent fragment analysis. In Figure 6A, a normal-appearing adjacent tissue specimen shows a single-peak of fluorescence signal at the RepIN20 microsatellite locus indicating homozygosity for this marker. Normal samples that are homozygous at a particular microsatellite marker cannot provide information of allelic change in the tumor; therefore they were not scored for LOH. In Figure 6B, both the PDAC tumor and its normal-appearing adjacent tissue shows a double-peak at the CAR/CAL microsatellite locus indicating heterozygosity for this marker, and a partial loss of the second peak is observed in the tumor sample.

As shown in Table 1, 8 out of 55 (14.5%) informative samples displayed LOH at the CAR/CAL locus, and 6 out of 56 (10.7%) informative samples displayed LOH at RepIN20. Of these, 4 samples displayed LOH at both loci. Totally LOH was seen in 10 samples. Of the 73 PDAC tumor samples in this study, 8 were homozygous at both microsatellite loci, so that the LOH information was obtained from only 65 samples. In total, 10 out of 65 (15.4%) of these PDAC tumor samples displayed LOH at one or both loci.

SEL1L LOH is not associated with its downregulation at the RNA level

SEL1L qPCR results were available for only 49 out of the 65 informative sample pairs due to the quality of the corresponding RNA samples. In the group of

samples displaying *SEL1L* LOH (total n = 8), 5 samples presented with *SEL1L* downregulation and 3 samples presented with normal *SEL1L* expression. In the group of samples without LOH (total n = 41), 24 samples presented with *SEL1L* downregulation and 17 with normal *SEL1L* expression. Using Fisher's exact test to evaluate the association between the presence of LOH in *SEL1L* gene region and the expression of *SEL1L* mRNA, LOH is not significantly associated with *SEL1L* downregulation ($P = 0.300$).

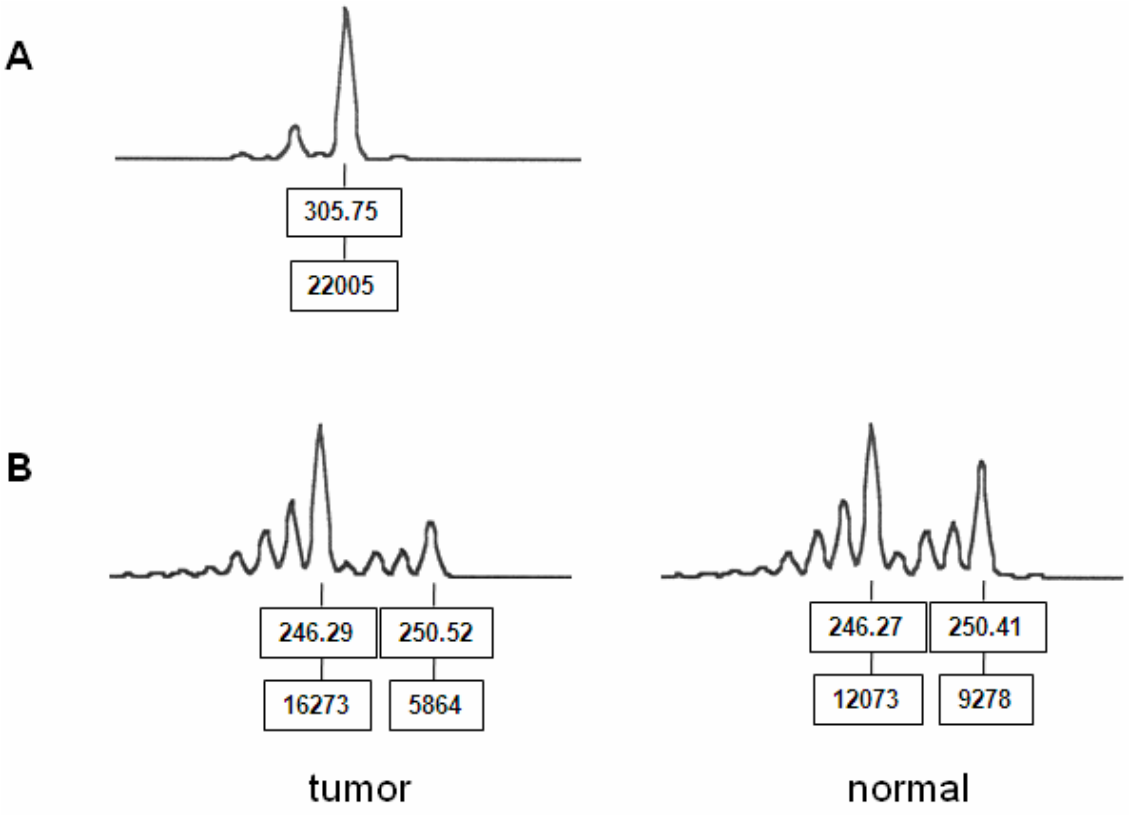

Figure 6. Chromatograms of fluorescent fragment analysis. Each peak has two labels: number in the upper box gives the length of the PCR fragment, and number in the lower box indicates the signal strength. **A.** Result for homozygous specimen. **B.** Heterozygosity in a tumor and in its paired normal-appearing adjacent tissue. Allelic loss can be seen at the second peak in the tumor.

Table 1. Allelic Ratio at *SEL1L* Microsatellite Loci in PDAC Tumors

Sample	CAR/CAL	RepIN20	Sample	CAR/CAL	RepIN20
T1	1.074	1.390	T38	1.02	homo
T2	1.067	homo*	T39	homo	0.977
T3	1.023	1.065	T40	1.068	0.999
T4	0.923	1.289	T41	homo	homo
T5	homo	homo	T42	0.872	**0.493**
T6	1.082	0.998	T43	1.074	0.990
T7	homo	1.062	T44	1.075	1.269
T8	homo	0.925	T45	**2.062**	0.907
T9	1.180	1.101	T46	**2.133**	**0.572**
T10	1.052	homo	T47	0.958	0.965
T11	0.978	1.065	T48	1.175	homo
T12	homo	homo	T49	0.815	0.951
T13	1.205	homo	T50	0.903	1.031
T14	1.051	0.967	T51	homo	homo
T15	0.960	1.081	T52	**1.992**	1.101
T16	0.871	homo	T53	homo	1.088
T17	homo	0.928	T54	**1.739**	0.880
T18	1.103	1.020	T55	homo	1.013
T19	homo	1.080	T56	1.179	1.292
T20	0.954	1.137	T57	1.263	1.033
T21	1.056	0.951	T58	**1.864**	**0.469**
T22	homo	homo	T59	0.921	1.049
T23	0.946	0.994	T60	1.316	0.796
T24	**1.803**	**1.641**	T61	0.96	1.107
T25	1.063	0.996	T62	**0.509**	**0.225**
T26	1.024	homo	T63	homo	0.999
T27	homo	homo	T64	0.973	homo
T28	1.117	1.128	T65	0.834	0.712
T29	homo	homo	T66	**0.544**	1.015
T30	0.956	1.010	T67	1.117	1.058
T31	homo	homo	T68	1.022	1.060
T32	homo	1.029	T69	0.953	1.158
T33	1.008	1.139	T70	1.097	1.002
T34	1.015	0.999	T71	1.005	1.045
T35	1.109	1.276	T72	0.946	homo
T36	0.955	0.714	T73	1.096	1.114
T37	homo	**3.480**			

* Homo – homozygous.
Number in bold indicates the presence of loss of heterozygousity.

2.4 Discussion

In this study, LOH was detected at two *SEL1L* intragenic microsatellite loci (CAL/CAR and RepIN20) in 15.4% of the PDAC tumors (Table 1). Fluorescent fragment analysis results showed an imbalanced relative intensity rather than total loss of one allele. Because of the heterogeneity of cancer cells, it is possible that LOH is not displayed in every single tumor cell but only in a sub-population of the cells. Also, because the samples that were studied were not from tissue micro-dissection, the tumor samples may contain some non-tumor tissue. Therefore, this may explain a partial allelic loss in the cases displaying LOH.

The results indicate that genome instability exists in the *SEL1L* gene region in a small portion of PDACs. Although it was not possible to determine the exact boundaries of the region of allelic loss by performing LOH analysis, the presence of LOH indicates that there is a genomic abnormality in the *SEL1L* gene region that could possibly lead to the production of aberrant SEL1L proteins.

In this study, there was no evidence showing that LOH correlated with SEL1L mRNA downregulation. This may be because one functional allele is sufficient to maintain the normal expression of *SEL1L*. However, even if the expression level of SEL1L mRNA is normal, if aberrant SEL1L proteins are generated, they may competitively interrupt the binding of normal SEL1L protein to the unfolded proteins for degradation.

Chapter 3

SEL1L CpG Island Methylation

3.1 Introduction

Gene promoter regions usually contain a cluster of cytosine-guanine dinucleotides (CpG) known as CpG islands. Hypermethylation of the cytosine residues in CpG sites may induce chromatin condensation and inhibit the binding of transcription factors, resulting in repression of gene expression [73, 74]. Aberrant CpG island methylation is a common epigenetic mechanism for transcriptional silencing of tumor suppressor genes [75]. Some of the most frequently reported genes that are silenced by DNA methylation include *CDKN2A/p16-INK4* in lung cancer, colorectal cancer, and gastric carcinoma [76-78]; Ras association domain family 1 (*RASSF1*) in gliomas, lung cancer, and ovarian cancer [79-81]; and O6-methylguanine-DNA methyltransferase (*MGMT*) in lung cancer and colorectal cancer [82, 83]. Aberrant promoter methylation of *p16-INK4* has been seen in 52% of PDAC cases [84]. Some other genes that have been found to display hypermethylation in PDAC include the multiple endocrine neoplasia I (MEN1) and serpin peptidase inhibitor B5 (SERPINB5) [85, 86].

In this chapter, the goal was to determine whether hypermethylation contributes to *SEL1L* downregulation.

3.2 Materials and Methods

Materials

DNA was extracted from 41 PDAC tumors and 6 PDAC cell lines. Of the cell lines, MDAPanc3, MDAPanc28 and MDAPanc48A were established in our laboratory, and Panc-1, Capan-2 and AsPC-1 cell lines were purchased from the American Type Culture Collection (ATCC, Manassas, VA).

Bisulfite DNA sequencing

The bisulfite (BS) modification method is commonly used to determine the pattern of DNA methylation. Sodium bisulfite is a chemical compound with the chemical formula $NaHSO_3$. It can deaminate cytosine into uracil, but does not affect the methylated form of cytosine with a methyl group attached to carbon 5 [87]. Therefore, the methylated and unmethylated cytosines can be distinguished from one another by using this method (Figure 7).

DNA samples were treated with BS using the EZ DNA Methylation Gold Kit (Zymo Research, Orange, CA). The treatment started from 1ug of genomic DNA in a 20µL reaction. The procedure was carried out according to the manufacturer's instructions. The modified *SEL1L* promoter region was amplified by PCR, and the PCR products were subsequently analyzed by either pyrosequencing or Sanger sequencing. Universal methylated DNA and universal unmethylated DNA (Zymo Research) were used as controls to assess the efficiency of BS-mediated conversion for both sequencing methods.

For pyrosequencing, nested PCR reactions were performed. The first set of PCR primers was SEL1Lmeth1 (forward 5′-GTT GAA TTT AGG GGT TAT TAA TTA GTT GGG-3′ and reverse 5′-TTC TAA TCC AAT CAC CAT AAT CTC CC-3′); and the nested primers were SEL1Lmeth2 (forward 5′-ATT TAG GGG TTA TTA ATT AGT TGG GGT T-3′ and reverse 5′-biotin-AAA ATC ATT CAT TAA CCA ATC ATT ATA C-3′). The sequencing primer was SEL1LmethS (5′-TTA GTT GGG GTT ATG-3′). Four CpG sites were included in the analyzed sequence, and the methylation status of these sites was evaluated for 24 of the PDAC tumors and 6 cell lines using the PSQ HS96A system (Biotage, Foxboro, MA) and the allele quantification module.

For Sanger sequencing, nested PCR was performed of the entire CpG island of *SEL1L.* The first set of primers was SEL1Lmeth3 (forward 5′-GAT GAG TTT TTT TTT TTT AGT TTT GGA TTT A-3′ and reverse 5′-TCC TAT ATC AAA ATT CAT TCC TTT AAA AT-3′), and the set of nested primers was SEL1Lmeth4 (forward 5′-ATT TAG GGG TTA TTA ATT AGT TGG GG-3′ and reverse 5′-CAC TCC ACC TTC CTA AAT AAC C-3′). The PCR products were purified with a QIAquick PCR Purification Kit (Qiagen) and then sequenced in the DNA Analysis Facility at UTMDACC using ABI PRISM 3730 DNA sequencers (Applied Biosystems, Foster City, CA). SEL1Lmeth4 reverse primer was used as sequencing primer. With this sequencing method, the methylation status of the 6 PDA cell line and 17 PDAC tumor DNAs were evaluated.

The PCR amplification was carried out in a final volume of 30 μL of a mixture containing 10 pmol of each primer, deoxynucleotide triphosphates (dNTP) each at

0.25 mM, KCl (50 mM), $MgCl_2$ (1.5 mM), Tris-HCl (10 mM, pH 8.3), and 1 unit of AmpliTaq Gold DNA Polymerase (Applied Biosystems). For the reactions using the first set of primers (SEL1Lmeth1 or SEL1Lmeth3), 2 ul of BS-treated DNA was added as template. For the reactions using the nested primers (SEL1Lmeth2 or SEL1Lmeth4), 1 ul of the PCR product from the first round was used as template. The reactions were started at 95°C for 5 minutes, followed by 40 cycles (95°C for 45 seconds, proper annealing temperature for 45 seconds, and 72°C for 45 seconds) and then an extension of 72°C for 7 minutes.

SEL1L CpG island sequences and locations of the primers are shown in Figure 8.

A.

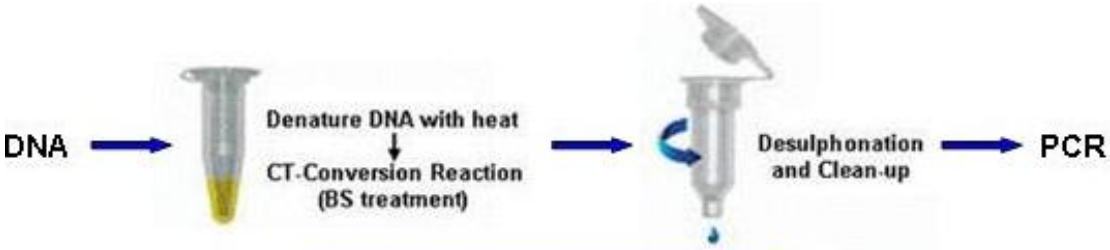

B.

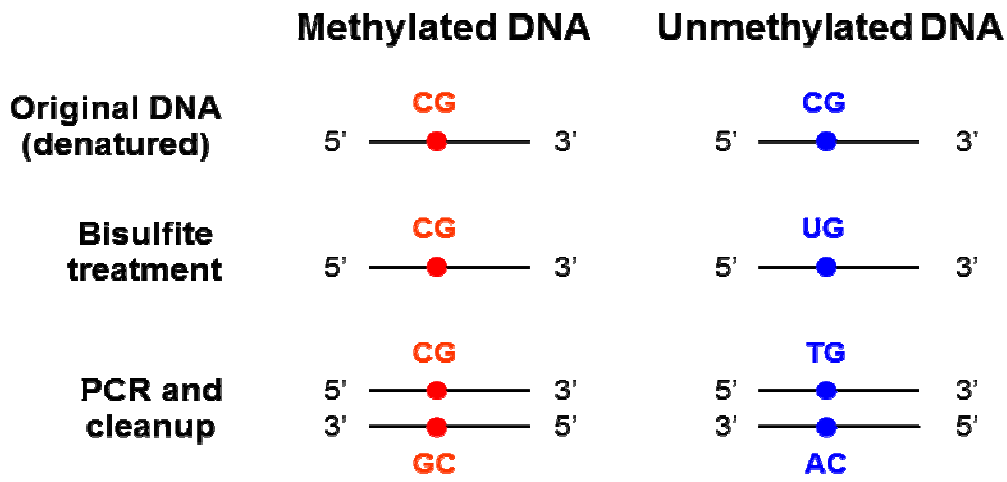

Figure 7. Bisulfite sequencing for methylation detection.

A. Bisulfite treatment flowchart (picture is modified from Zymo Research company website); **B.** Sequence after BS treatment at CpG site for methylated and unmethylated DNA.

ctgggaattgtagtctcggatgagcctctttctcccagtcttggactcacgcgctgattc

TTGGGAATTGTAGTTTCGGATGAGTTTTTTTTTTTTAGTTTTGGATTTACGCGTTGATTT

SEL1Lmeth3F

cggttgaacccaggggctaccaattagctggggccatgtccgtgagtcgtggtccaaccg

CGGTTGAATTTAGGGGTTATTAA*TTAGTTGGGGTTTATG*TTCGTGAGTCGTGGTTTAATCG

SEL1Lmeth1F SEL1Lmeth4F SEL1Lmeth2F

agaaagctggtgtgggagcttcgtacaatgattggccaatgaatgaccccggggcggag

AGAAAGTTGGTGTGGGAGTTTCGTATAATGATTGGTTAATGAATGATTTTCGGGGCGGAG

SEL1Lmeth2R

caatgggggtgggcggggagaccatggtgattggaccagaagcccgcgacggcgggcggg

TAATGGGGGTGGGCGGGGAGATTATGGTGATTGGATTAGAAGTTCGCGACGGCGGGCGGG

SEL1Lmeth1R

gattggctgcgcgctgggtcagggaagcctgggaaggggcggaggaaggagactagagca

GATTGGTTGCGCGTTGGGTTAGGGAAGTTTGGGAAGGGGCGGAGGAAGGAGATTAGAGTA

ggaagagcagcggcgaggcggcggtggtggctgagtccgtggtggcagaggcgaaggcga

GGAAGAGTAGCGGCGAGGCGGCGGTGGTGGTTGAGTTCGTGGTGGTAGAGGCGAAGGCGA

cagctctaggggttggcaccggccccgagaggaggatgcgggtccggatagggctgacgc

TAGTTTTAGGGGTTGGTATCGGTTTCGAGAGGAGGATGCGGGTTCGGATAGGGTTGACGT

tgctgctgtgtgcggtgctgctgagcttggcctcggcgtcctcgggtcagtatccgcccc

TGTTGTTGTGTGCGGTGTTGTTGAGTTTGGTTTCGGCGTTTTCGGGTTAGTATTCGTTTT

ctcgggctgaaggcccagagcctccgccccccagcctctacagccggcggggccgtgggg

TTCGGGTTGAAGGTTTAGAGTTTTCGTTTTTTAGTTTTTATAGTCGGCGGGGTCGTGGGG

actccaggctcgggaccccgttctccctgggcacatctcgcactgggctgtcactcgctc

ATTTTAGGTTCGGGATTTCGTTTTTTTTGGGTATATTTCGTATTGGGTTGTTATTCGTTT

tttggctttgcttggcctgcgccaaaggggctatttaggaaggtggagtggggtggaaaa

TTTGGTTTTGTTTGGTTTGCGTTAAAGGGGTTATTTAGGAAGGTGGAGTGGGGTGGAAAA

SEL1Lmeth4R

agaaggggcggtcaccctgcccacacctctctcccacgtaacaaactttgcgcgactctt

AGAAGGGGCGGTTATTTTGTTTATATTTTTTTTTTACGTAATAAATTTTGCGCGATTTTT

ctcacgaacgcggaattgactccaaaggaatgaatcctgatacaggagcccgagtggagc

TTTACGAACGCGGAATTGATTTTAAAGGAATGAATTTTGATATAGGAGTTCGAGTGGAGT

SEL1Lmeth3R

Figure 8. *SEL1L* CpG island sequences and locations of BS PCR primers.

Yellow highlight: *SEL1L* CpG island; Lower case: original sequence before BS treatment; Upper case: converted sequence after BS treatment; Underline: CpG site; Red rectangle: primers for BS pyrosequencing PCR; Blue rectangle: primers for BS Sanger sequencing PCR; Italic: SEL1LmethS.

3.3 Results

Methylation is not detected in the SEL1L *promoter CpG island*

BS sequencing results of the universal unmethylated control showed complete conversion of all the cytosine residues, and the universal methylated control showed conversion of all the cytosine residues except for those at the CpG sites. These results indicated that the BS treatment worked successfully and could detect the methylation status of *SEL1L* CpG island reliably.

The BS pyrosequencing method examined 3 CpG sites with high fidelity in the *SEL1L* promoter region. All of the samples analyzed by this method presented with 100% of thymine (T) and 0% of cytosine (C) at the covered CpG sites, which indicated a lack of methylation at these sites. Sanger sequencing of BS-treated DNA also did not display evidence for methylation at the examined CpG sites in any of the samples. Representative results of both sequencing methods are shown in Figure 9.

A.

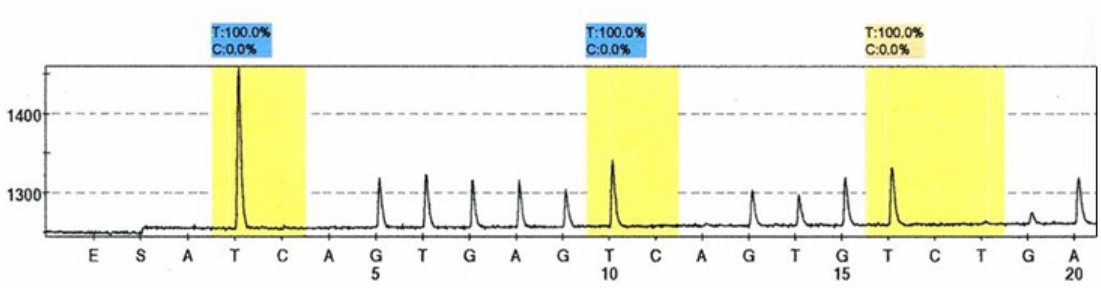

B.

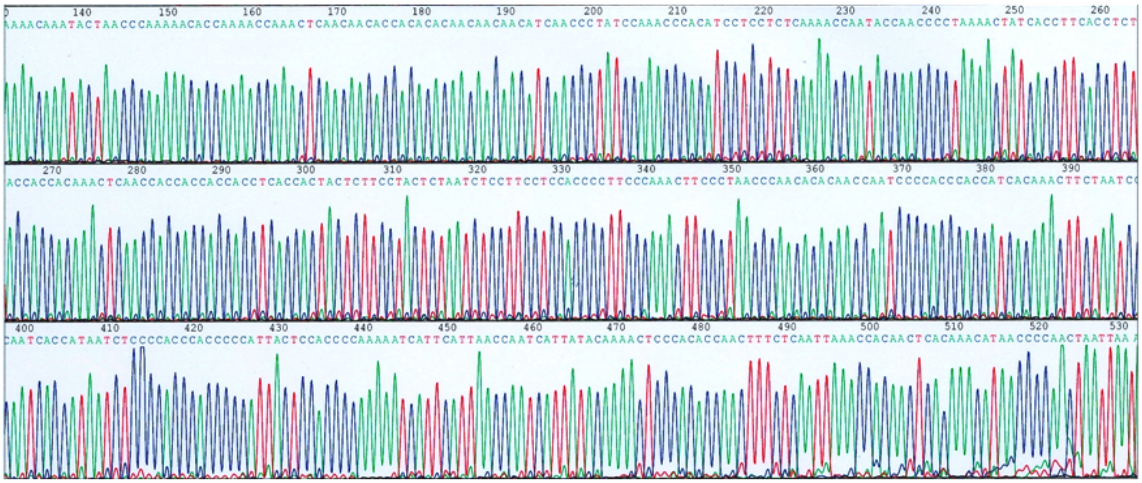

Figure 9. Bisulfite sequencing results.

A. Pyrosequencing chromatogram indicating that at all three CpG sites the cytosines were 100% unmethylated; D. Sanger sequencing chromatogram showing a sequence from reverse direction without methylation.

3.4 Discussion

The advantage of the pyrosequencing method is that it is quantitative, so it was possible to determine if the levels of hypermethylation detected in the tumor tissues were greater than in the normal adjacent tissues by comparing the cytosine/thymine ratio. The disadvantage of this method was that only a few of the CpG sites in one run could be detected which might not represent the whole CpG island.

The advantage of the Sanger sequencing method was that the methylation status of the whole CpG island could be evaluated. The disadvantage was that after bisulfite treatment, the converted DNA might contain poly T or poly A. When the poly T/A sequences are too long, it would be difficult to sequence by this method. Sanger sequencing without cloning only gives information about the average product. To get statistically meaningful data commonly cloning and sequencing individual molecules are needed.

Both of the sequencing methods were used for this study as they are complementary to each other and the results using one method can be confirmed by the other. The results suggest that hypermethylation is not a mechanism of *SEL1L* downregulation. However, in some rare cases, alternate promoters containing CpG islands may exist in or around some genes which can also regulate gene expression. This possibility can be further studied for the *SEL1L* gene.

Chapter 4

SEL1L and MicroRNA

4.1 Introduction

MiRNAs are endogenous non-coding RNAs ~ 18–24 nucleotides long. Generally, miRNAs bind to the 3′ untranslated region (UTR) of their target genes through imperfect complementation and repress gene expression either by increasing mRNA degradation or by inhibiting translation [88]. Whether the binding of miRNA drives mRNA degradation or translational inhibition of the target gene depends on the structure of the miRNA–mRNA duplex. Many studies have reported that miRNA may repress target gene translation even when it does not affect the mRNA level [89].

Emerging evidence shows that deregulated miRNAs may play an oncogenic or tumor-suppressive role in different kinds of cancers by repressing the expression of oncogenes or tumor suppressor genes [90, 91]. In PDAC, it has been reported that microRNA-155 inhibits the expression of tumor suppressor gene tumor protein 53-induced nuclear protein 1 (TP53INP1), and microRNA-21 regulates the expression of the tumor suppressor programmed cell death 4 (PDCD4) [92, 93]. Because miRNAs can be shed into the serum and be isolated and studied, they may serve as biomarkers for early detection and diagnosis of cancers, and for evaluating patients' prognoses [94]. In addition, the functional involvement of these miRNAs in tumorigenesis makes them potential therapeutic targets for the treatment of PDAC [95, 96].

The 3′ UTR of the *SEL1L* gene is larger than 4000 bp and thus provides great potential to bind miRNAs. Using miRNA microarrays, three studies have investigated the genome-wide alterations in miRNA expression found in PDAC [97-99]. There are 18 miRNAs that displayed upregulation in PDAC in at least two of these studies. In this study, I sought to determine whether these aberrantly upregulated miRNAs are

responsible for *SEL1L* downregulation in PDAC using both statistical and functional analysis.

4.2 Materials and Methods

Materials

RNA samples from a total of 42 tumor/normal pairs were examined using qPCR. Protein samples from 40 out of the 42 pairs have been used for Western blotting. MDAPanc3, MDAPanc28, MDAPanc48A and MDAPanc48B cell lines were established in our laboratory, all other cell lines used in this study were purchased from ATCC.

Extraction of DNA, RNA, and Protein

Total RNA including miRNA extraction and DNA extraction have been previously described in the Methods section in Chapter 1. Protein was isolated from the phenol–ethanol supernatant obtained after precipitation of the RNA and DNA. Protein concentrations were determined with the bicinchoninic acid (BCA) protein assay reagents (Pierce, Rockford, IL).

MiRNAs predicted to target **SEL1L**

The microRNA.org resource (miRanda) was searched to identify which of the 18 aberrantly upregulated miRNAs were predicted to target *SEL1L*. MiRanda is a comprehensive resource for miRNA target predictions that computes the optimal sequence complementarity between a mature miRNA and an mRNA using a weighted dynamic programming algorithm [100]. From the search, 7 miRNAs were identified that potentially target *SEL1L*: hsa-mir-143, hsa-mir-155, hsa-mir-181a, hsa-mir-181c,

hsa-mir-205, hsa-mir-210, and hsa-mir-223. The predicted binding sites and the chromosomal locations of these miRNAs are shown in Table 2.

Table 2. Predicted Binding Sites to *SEL1L* and Chromosome Locations of 7 MiRNAs

Name	Binding Site [a]	Location
hsa-mir-143	3' CUCGAUGUCACGAAGUAGAGU 5' miRNA 3690: 5' UAUGUGCAGGGAAUCAUCUCA 3' *SEL1L*	5q32
hsa-mir-155	3' UGGGGAUAGUGCUAAUCGUAAUU 5' miRNA 1186: 5' CAUUUUCUCACUGUUAACAUUAG 3' *SEL1L*	21q21.3
hsa-mir-181a	3' UGAGUGG--CUGUCGCAACUU ACAA 5' miRNA 179: 5' UCUUACCUAAACUGAGCUGAAUGUU 3' *SEL1L*	9q33.3
hsa-mir-181c	3' UGAGUGG--CUGUC-CAACUU ACAA 5' miRNA 179: 5' UCUUACCUAAACUGAGCUGAAUGUU 3' *SEL1L*	19q13.13
hsa-mir-205	3' GUCUGAGGCCACCU-UACUUCCU 5' miRNA 1551: 5' UAGUCUAUAAUGAACAUGAAGGC 3' *SEL1L*	1q32.2
hsa-mir-210	3' AGUCGGCGACAGUGUGCGUGUC 5' miRNA 3256: 5' GACUAACAUUUCACAUGCACAU 3' *SEL1L*	11p15.5
hsa-mir-223	3' ACCCCA UAAACUGUUUGACUGU 5' miRNA 709: 5' GCAAAACCUUG-UGAACUGACU 3' *SEL1L*	Xq12

[a] The binding sites were identified using the microRNA.org resource. The numbers before the *SEL1L* 5' end represent the nucleotide position on the *SEL1L* 3' untranslated region. A solid line between a miRNA and *SEL1L* indicates a complementary pairing. A broken line indicates a G-U wobble pairing.

qPCR

Assessment of *SEL1L* mRNA expression has been described in the Methods section in Chapter 2. The expression levels of the 7 mature miRNAs were examined in the DNA Analysis Facility at UTMDACC. The TaqMan MicroRNA Assay kits individually targeting the 7 miRNAs (Applied Biosystems) were used for the assays. RNA from the matched normal-appearing adjacent tissue was used as a calibrator for the tumor. Expression of the miRNAs was normalized to that of U6B small nuclear RNA (RNU6B). All of the assays were run in duplicate and an average RQ was calculated as final result. Again, a gene was considered to be upregulated if RQ $\geq$ 2, and was considered to be downregulated if RQ $\leq$ 0.5.

Western blotting

Thirty micrograms of each of the protein samples were resolved on 10% sodium dodecyl sulfate polyacrylamide gel electrophoresis (SDS-PAGE). Then proteins were transferred to 0.45 μM nitrocellulose membrane (Bio-Rad Laboratories, Hercules, CA). A goat polyclonal antibody to SEL1L (Santa Cruz Biotechnology, Santa Cruz, CA) was used at 0.8 μg/mL in tris-phosphate buffered saline (TPBS) with 5% Blotto (GE Healthcare, Piscataway, NJ). Bovine anti-goat immunoglobulin G-horseradish peroxidase (IgG-HRP) secondary antibody (Santa Cruz Biotechnology) was used at a dilution of 1:5000**.** TPBS with 0.2% Tween20 (Sigma-Aldrich, St. Louis, MO) was used as washing buffer to reduce the high background of non-specific blotting when using a goat antibody. The membrane was washed 3 times for 15 minutes following antibody incubation. The *GAPDH* antibody (Abcam, Cambridge,

MA) was used as a loading control at a concentration of 0.4 μg/mL. Goat anti-rabbit IgG-HRP (Santa Cruz Biotechnology) was used as a secondary antibody to GAPDH at a dilution of 1:5000. The membrane was washed in TPBS with 0.05% Tween20 3 times for 10 minutes following the antibody incubation.

Amersham ECL Plus Western Blotting Detection Reagents (GE Healthcare) were used to detect the signals. The intensity of the bands on Western blots was measured with Quantity One version 4.6.1 analysis software (Bio-Rad Laboratories). Desired bands from two exposure times (20 seconds and 1 minute) were quantified, and their average intensities were calculated. The RQ of SEL1L protein expression in the tumor was normalized to that of GAPDH and compared with that of the matched normal-appearing adjacent tissue.

Statistical analysis

The Fisher's exact test was used to evaluate the association between the expression levels of *SEL1L* mRNA and the miRNAs. The Kruskal–Wallis test was used to evaluate expression differences between the groups with 0, 1, 2, or 3 upregulated miRNAs. Pearson's correlation coefficient was used to measure the correlation between *SEL1L* mRNA expression and SEL1L protein expression in PDAC tumors. All tests of statistical significance were 2-sided. $P < 0.05$ was considered statistically significant. All statistical analyses were performed using Stata version 10.1 software (Stata, College Station, TX).

Cell culture

The PDAC cells, including Panc1, BxPC3, MiaPaCa2, ASPC1, Capan1, Capan2, PL3, PL18, MDAPanc3, MDAPanc28, MDAPanc48A and MDAPanc48B, as well as Human Embryonic Kidney (HEK) 293T cells were maintained at 37°C and 5% CO2 in Dulbecco's Modified Eagle Medium: Nutrient Mixture F-12 (DMEM/F12) (Mediatech, Manassas, VA) supplemented with 10% fetal bovine serum (FBS) (Gemini Bio-Products, West Sacramento, CA) and 1% penicillin/streptomycin (Mediatech). The hTERT-HPNE cells were cultured in 75% DMEM without glucose (Mediatech), 25% Medium M3 Base (Incell Corporation, San Antonio, TX) supplemented with 10 ng/ml human recombinant EGF (Sigma-Aldrich), 5.5 mM D-glucose (Mediatech), 5% FBS and 0.75% puromycin (Mediatech)**.**

Luciferase assay

The pMIR-REPORT miRNA Expression Reporter Vector System (Applied Biosystems) was used to determine whether the miRNAs bind to the predicted binding sites and regulate reporter expression. The pMIR-REPORT Luciferase Reporter Vector may produce high-level expression of firefly luciferase under the control of a mammalian promoter/terminator system. The miRNA target cloning region is located downstream, i.e. 3' UTR, of the luciferase sequence. The predicted *SEL1L*–miRNA binding sites and more than 100 bp of flanking sequence at both the 5' and 3' ends were inserted into the cloning region. Because the putative binding sites for hsa-mir-155 and hsa-mir-223 are very close to each other, a construct containing the putative binding sites for both of the miRNAs was established (Figure 10). The 100 bp flanking sequences help to ensure that the secondary structure of the binding sites will

not be interrupted and thus better represent the *in vivo* condition. A second vector, pMIR-REPORT Beta-galactosidase (ß-gal) Reporter Vector, was used for normalization of transfection efficiency. A relative expression of the firefly luciferase was calculated by comparing that to the expression of ß-gal signal. For example, the average reading of the firefly luciferase signal in a sample was 6288437 and the average reading of the ß-gal signal in this sample was 47494, so the relative expression of the firefly luciferase was 6288437 / 47494 = 132.40.

A.

CTGAGAAACTCTTACCAGTCCACATGCAATTAGACATATTCAGCATATTTGTTATTTTAAAAGGGAGGG

TTGGGAGGTTTCTTATTGGTGATTGTCACACGGTATACCATACTCCTCTCCTTCAAAGAATGAAAGGCC

TTGTTAAGGAGTTTTTTGTGAGCTTTACTTCTTTGGAATGGAATATACTTATGCAAAACCTTGTGAACT

GACTCCTTGCACTAACGCGAGTTTGCCCCACCTACTCTGTAATTTGCTTGTTTGTTTTGAATATACAGA

GCCTTGATCCAGAAGCCAGAGGATGGACTAAGTGGGAGAAATTAGAAAACAAAACGAACTCTGGTTGGG

GTACTACGATCACAGACACAGACATACTTTTCCTAAAGTTGAAGCATTTGTTCCCAGGATTTATTTTAC

TTTGCATTTCTTTTTGCACAAAGAACACATCACCTTCCTGAATTCTTTAAATATGAAATATCATTGCCA

GGGTATGGCTTACAGTGACTACTATTATAATACTAAAACTCAGAGAATCAAAGATGGATTAAACTCAGT

GGTTGATGAAAGCCAAAACCTGTTTGTACTGTTCTATACTATTCAGGTATCTTTTTATTTCTGATAGTT

TTATATTATAATAGAAAGCCAGCCACTGCTTAGCTATCATAGTCACCATTTTCTCACTGTTAACATTAG

GAAAATCAAGGCTACTATGCTTCAGGATTGTCTGGTTAAATAGTATGGGAAAAAAACTGAAGAGTTTCA

CATAATTACACACGTGAAATAATTAAAGCTT

B.

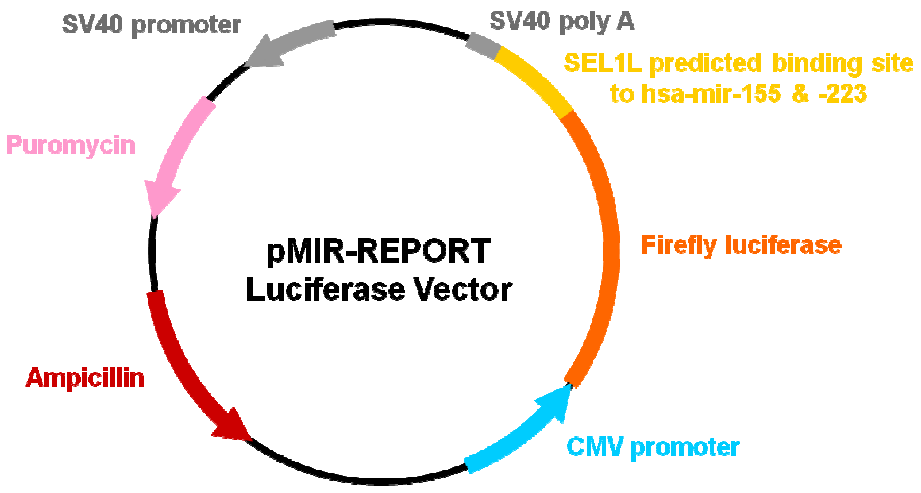

Figure 10. pMIR-REPORT Luciferase Reporter construct containing predicted binding sites of *SEL1L* to hsa-mir-155 and hsa-mir-223. A. Sequence that was inserted into the vector. Yellow highlight: hsa-mir-223 binding site; Red highlight: hsa-mir-155 binding site. **B.** Schematic diagram of the construct.

MDAPanc3 cells, PL18 cells or BxPC2 cells were plated in 6-well plates and reached a cell confluency of 50%-60% at the time of transfection. In each well, a mixture of 1.5 ug of Luciferase Reporter plasmid DNA (with or without the binding sites) and 0.15 ug of ß-gal Reporter plasmid DNA was transfected into the cells with 5 ul of Lipofectamine LTX (Invitrogen) and 1.65 ul of PLUS reagent (Invitrogen). Cells were washed with PBS twice and collected after 24 hours and 48 hours. Firefly luciferase activity and ß-gal activity were determined by using the Dual-Light Luciferase and ß-Galactosidase Reporter Gene Assay System (Applied Biosystems) according to the manufacturer's instructions. A 20/20n Single Tube Luminometer (Turner Biosystems, Sunnyvale, CA) was used for the measurements. All of the transfections were performed in triplicate and the average activities were calculated. Then the firefly luciferase activities were normalized to ß-gal activity.

293T cells were plated in 24-well plates and transfected at a cell confluency of 80-90%. The cells were transfected with 200 ng of Luciferase Reporter plasmid DNA (with or without the binding sites), 5ng of ß-gal Reporter plasmid DNA, and 5 pmol of miRNA precursor or negative control (final concentration 25 nM) using 2 ul of Lipofectamine2000 (Invitrogen). The miRNA precursors and negative control (miR-control) were purchased from Ambion/Applied Biosystems. The miRNA precursors are synthetic, chemically modified double-stranded RNA molecules that mimic endogenous mature miRNAs. The negative control is similar to the miRNA precursor with a random sequence that has been validated not to produce identifiable effects on known miRNA function. Cells were harvested after 48 hours of the co-transfection. Firefly luciferase activity and ß-gal activity were assessed as described in the last

paragraph.

MiRNA inhibition and overexpression

Chemically modified antisense oligoribonucleotides, termed "antagomirs", were used in this study to inhibit hsa-mir-155 and hsa-mir-223. Antagomirs have been reported to specifically, efficiently reduce the expression of corresponding miRNAs [101]. The antagomir against hsa-mir-155 is: 5'-mA*mC*mCmCmCmUmAmUmC-mAmCmGmAmUmUmAmG-mCmAmU*mU*mA*mA*/Chol-3'. The antagomir against hsa-mir-223 is: 5'-mU*mG*mGmGmGmUmAmUmUmUmGmAmCmAmA mAmCmUmG*mA*mC*mA*/Chol-3'. The negative control for the antagomirs is: 5'-mA*mA*mGmUmGmGmAmUmAmUmUmGmUmUmGmCmCmA*mU*mC*mA*/ Chol-3'. The lower case "m" represents 2'-O-methyl-modification; the asterisk (*) represents a phosphor-rothioate linkage; and "Chol" represents cholesterol linked through a hydroxyprolinol linkage. The negative control is a random sequence that has been validated by Ambion not to inhibit any known miRNA function. These antagomirs were synthesized and then purified by high-performance liquid chromatography (Integrated DNA Technologies, Coralville, IA).

BxPC3, PL18 or Capan2 cells were plated in 6-well plates and reached a cell confluency of 50%-60% at the time of transfection. In each well, 200 pmol of the antagomir or negative control (final concentration 200 nM) was transfected into the cells with 2 ul of Oligofectamine (Invitrogen). For PL18 cells, after 24 hours of transfection, a double knockdown was performed by transfecting the same amount of hsa-mir-155 antagomir into the cells again.

Ambion miRNA precursors and negative control were used for the overexpression study of the miRNAs of interest. MDAPanc3 or Miapaca2 cells were plated on 6-well plates and reached a cell confluency of 50%-60% at the time of transfection. In each well, 30 pmol of miRNA precursor or negative control (final concentration 30 nM) was transfected into the cells using 2 ul of Oligofectamine (Invitrogen).

The cells mentioned above were washed with PBS twice and collected after 24 hours, 48 hours and 72 hours. Then total RNA and protein were extracted for qPCR and Western blotting as described previously. Proteins also were extracted by lysing the cells in Radio-Immunoprecipitation Assay (RIPA) buffer (Sigma-Aldrich).

Reverse phase protein assay (RPPA)

The cell lysates were denatured with 1% SDS (with beta-mercaptoethanol) and diluted in five 2-fold serial dilutions in lysis buffer containing 1% SDS. Serial diluted lysates were arrayed on nitrocellulose-coated slides (Grace Bio-lab, Bend, OR) using an Aushon 2470 Arrayer (Aushon BioSystems, Billerica, MA). Each slide was probed with validated primary antibodies plus biotin-conjugated secondary antibodies. A total of 172 antibodies including 23 replicated antibodies were included in the data set (SEL1L antibody was not available for this experiment). All the proteins assessed are related to cancer pathogenesis. Each array included spots corresponding to positive and negative controls prepared from mixed cell lysates or dilution buffer, respectively. The signal obtained was amplified using a Dako Cytomation–catalyzed system (Dako, Carpinteria, CA) and visualized by diaminobenzidine (DAB) colorimetric reaction.

The slides were scanned, analyzed, and quantified using a customized-software Microvigene (VigeneTech Inc., Carlisle, MA) to generate spot intensity. Protein levels for each sample were determined by interpolation of each dilution curve into a logistic model, Supercurve Fitting, developed by the Department of Bioinformatics and Computational Biology at UTMDACC [102]. This model fits a single curve using all the dilution series on a slide with the signal intensity as the response variable and the dilution steps as independent variables. The protein concentrations of each set of slides were then normalized by median polish, which was corrected across samples by the linear expression values using the median expression levels of all antibody experiments to calculate a loading correction factor for each sample. A relative protein expression level was calculated by comparing the normalized linear value in the sample transfected with miRNA precursor to that in the sample transfected with negative control at the same time point. A protein was considered to be upregulated if $RQ \geq 1.500$, and to be downregulated if $RQ \leq 0.667$.

Ingenuity pathways analysis (IPA)

The "Core Analysis" function in IPA (Ingenuity System Inc, Redwood City, CA) was used to interpret the RPPA data for pathways and networks involved [103]. Molecules from the data set that displayed expression variation and were contained in the Ingenuity Knowledge Base were analyzed. The significance of the association between the data set and the canonical pathway was measured by Fisher's exact test to calculate a *P*-value. These molecules were also overlaid onto a global molecular

network developed from information in the Ingenuity Knowledge Base, and networks were then algorithmically generated based on their connectivity.

4.3 Results

Expression levels of hsa-mir-143, hsa-mir-155, and hsa-mir-223 are inversely correlated with* SEL1L *mRNA expression in PDAC tumors

Results from quantitative RT-PCR indicated that *SEL1L* mRNA was downregulated in 55% of the PDAC tumors, whereas the 7 miRNAs were upregulated in the following percentages of the PDAC tumors: hsa-mir-155, 52%; hsa-mir-205, 45%; hsa-mir-210, 45%; hsa-mir-181c, 40%; hsa-mir-143, 38%; hsa-mir-181a, 35%; and hsa-mir-223, 33% (Figure 11).

The RQs of the expression of *SEL1L* mRNA and the 7 miRNAs were initially assessed in 20 pairs of PDAC tumors and normal-appearing adjacent tissues by qPCR. The preliminary data showed that only levels of hsa-mir-143, hsa-mir-155, and hsa-mir-223 correlated significantly with *SEL1L* mRNA expression. Subsequent analyses of an additional 22 pairs of samples for these 3 miRNAs corroborated these findings, and the combined data from a total of 42 samples pairs are presented in Table 3.

The downregulation of *SEL1L* mRNA was found to be significantly associated with the upregulation of hsa-mir-143, hsa-mir-155, and hsa-mir-223 as evaluated using Fisher's exact test ($P < 0.0001$, $P < 0.0001$, and $P = 0.002$, respectively). As shown in Table 3, of the samples in which these miRNAs were upregulated, 14 (88%) out of 16, 18 (82%) out of 22, and 12 (86%) out of 14, respectively, showed *SEL1L* mRNA downregulation. Furthermore, of the 23 tumor samples in which *SEL1L* mRNA was downregulated, 20 (87%) displayed upregulation of at least 1 of these 3 miRNAs. The other 4 miRNAs (hsa-mir-181a, hsa-mir-181c, hsa-mir-205, and hsa-

mir-210) did not show a significant correlation with *SEL1L* mRNA expression (P = 0.749, P = 0.763, P = 0.654, and P = 0.469, respectively).

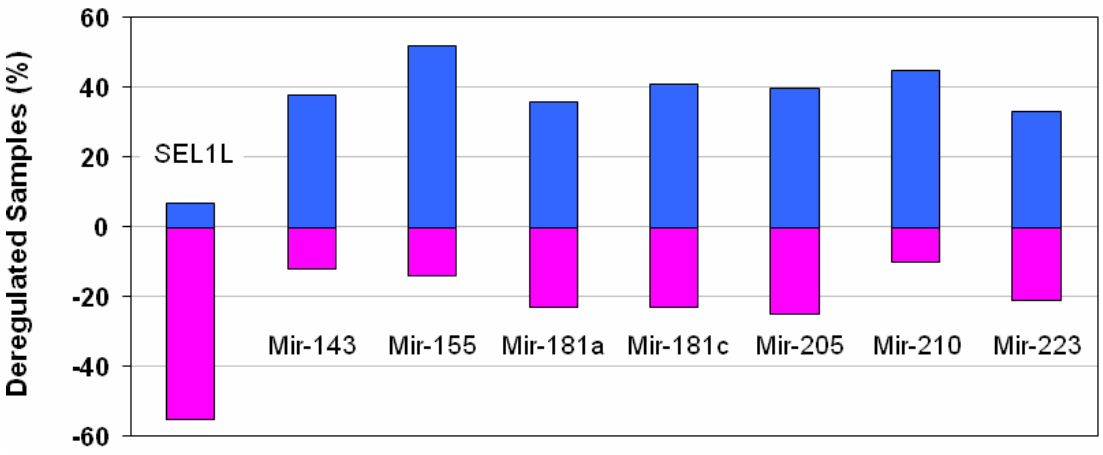

Figure 11. Percentage of the deregulation of *SEL1L* mRNA and 7 miRNAs in PDAC tumors.

Blue columns indicate gene upregulation. Pink columns indicate gene downregulation.

Table 3. Expression of *SEL1L* mRNA and 7 miRNAs in PDAC Tumors

A

MiRNA		Total n = 42 [a] *SEL1L* down (n = 23)	*SEL1L* normal (n = 16)	*SEL1L* up (n = 3)	Fisher's Exact Test
hsa-mir-143	**up** [b] (n = 16)	14	1	1	$P < .0001$
	normal (n = 20)	8	12	0	
	down (n = 6)	1	3	2	
hsa-mir-155	**up** (n = 22)	18	4	0	$P < .0001$
	normal (n = 15)	4	10	1	
	down (n = 5)	1	2	2	
hsa-mir-223	**up** (n = 14)	12	2	0	$P = .002$
	normal (n = 19)	8	11	0	
	down (n = 9)	3	3	3	

B

MiRNA		Total n = 20 *SEL1L* down (n = 11)	*SEL1L* normal (n = 7)	*SEL1L* up (n = 2)	Fisher's Exact Test
hsa-mir-181a	**up** (n = 7)	4	3	0	$P = .749$
	normal (n = 8)	5	2	1	
	down (n = 5)	2	2	1	
hsa-mir-181c	**up** (n = 8)	5	3	0	$P = .763$
	normal (n = 7)	4	2	1	
	down (n = 5)	2	2	1	

C

MiRNA		Total n = 20 *SEL1L* down (n = 11)	*SEL1L* normal (n = 9)	*SEL1L* up (n = 0)	Fisher's Exact Test
hsa-mir-205	**up** (n = 9)	5	4	0	$P = .654$
	normal (n = 8)	3	5	0	
	down (n = 3)	3	0	0	
hsa-mir-210	**up** (n = 9)	6	3	0	$P = .469$
	normal (n = 9)	3	6	0	
	down (n = 2)	2	0	0	

[a] Data in panels A, B, and C resulted from different sets of samples, which were randomly grouped.
[b] Up: RQ ≥ 2; normal: 0.5 < RQ < 2; down: RQ ≤ 0.5.

Inverse correlation between miRNA expression and SEL1L expression

As shown in Figure 12, the samples were divided into 4 groups on the basis of the number (0, 1, 2, or 3) of upregulated miRNAs in each sample. Because only hsa-mir-143, hsa-mir-155, and hsa-mir-223 showed correlations with *SEL1L* mRNA expression, this study was focused on the upregulation of these 3 miRNAs. The RQs of *SEL1L* mRNA expression in the tumors were compared for the groups. It was determined that as the number of overexpressed miRNAs increased, the median RQ of *SEL1L* mRNA expression decreased. The RQs of *SEL1L* mRNA expression among the four groups were significantly different ($P = 0.004$), and the trend of an increasing number of upregulated miRNAs corresponding to decreasing expression of *SEL1L* mRNA was also significant ($P_{trend} = 0.001$).

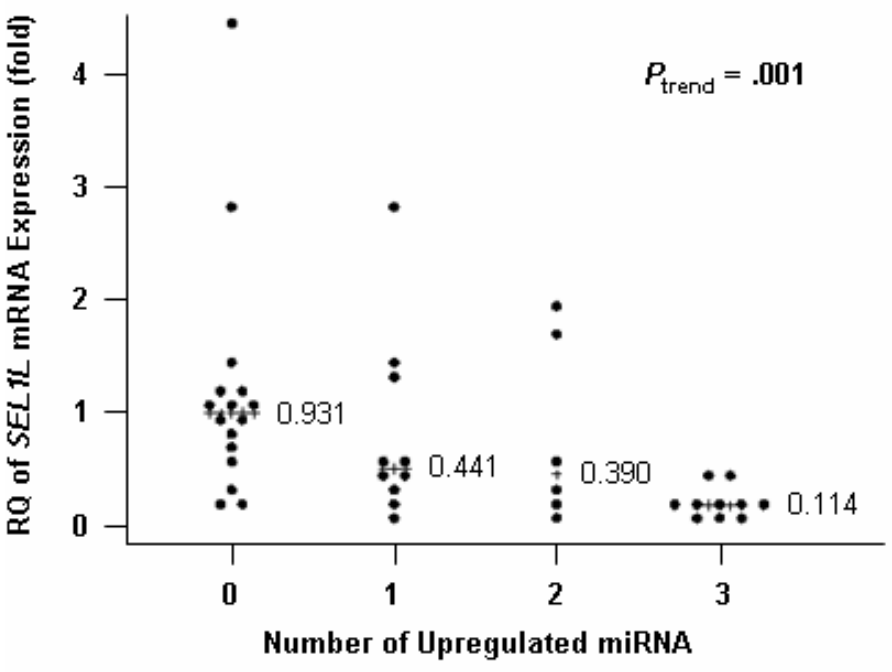

Figure 12. RQ of *SEL1L* mRNA expression in PDAC tumors plotted against the number of upregulated miRNAs.

Each horizontal line of pluses (+) and the number next to it represent the median fold change in *SEL1L* mRNA expression for that number of upregulated miRNAs.

The expression levels of hsa-mir-143, hsa-mir-155, and hsa-mir-223 are significantly associated with each other

The pairwise association was also evaluated between hsa-mir-143, hsa-mir-155, and hsa-mir-223 using Fisher's exact test (Table 4). Of the 42 tumor samples, 26 (62%) showed the same trend of expression between hsa-mir-143 and hsa-mir-155, 25 (60%) between hsa-mir-143 and hsa-mir-223, and 24 (57%) between hsa-mir-155 and hsa-mir-223. They were all significantly associated with each other (P = 0.015, P = 0.003, and P = 0.010, respectively).

Table 4. Relationships Between the Expression of 3 miRNAs in 42 PDAC Tumors

MiRNAs	Both up [a]	Both normal [b]	Both down [c]	Others [d]	Fisher's Exact Test
hsa-mir-143 & -155	13	11	2	16	P = .015
hsa-mir-143 & -223	13	10	2	17	P = .003
hsa-mir-155 & -223	10	12	2	18	P = .010

[a] Both of the miRNAs were upregulated in a tumor sample; [b] both of the miRNAs displayed normal expression; [c] both of the miRNAs were downregulated; [d] the miRNAs had a relationship other than these three kinds.

SEL1L protein expression correlates significantly with* SEL1L *mRNA expression

Because miRNAs may block target gene translation directly [88], SEL1L protein expression levels were assessed to determine whether the protein levels parallel the mRNA levels or whether the proportion of downregulation in PDAC tumors is greater at the protein level than at the mRNA level. The results are shown in Table 5**.** For both *SEL1L* mRNA and SEL1L protein, again the RQs of 2 and 0.5 were used as the cutoff values for considering a gene to be up- and downregulated. In those samples where the mRNA and the protein showed different trends of expression, Western blotting was repeated and the average RQ was calculated as the final result.

Of the 40 PDAC tumor samples listed in Table 5, it was determined that unlike *SEL1L* mRNA that was downregulated in 21 (53%) of the PDAC tumors, SEL1L protein was downregulated in only 16 (38%). In these 16 tumors, *SEL1L* mRNA was always downregulated. *SEL1L* mRNA and SEL1L protein displayed the same trends of expression (both up, both down, or both normal) in 32 (80%) of the 40 cases. The representative results of Western blotting are shown in Figure 13A. Pearson's correlation test showed that the RQ of SEL1L protein expression varied directly with the RQ of *SEL1L* mRNA expression and was statistically significant (Figure 13B).

Table 5. RQs of the Expression of *SEL1L* mRNA and SEL1L Protein in 40 PDAC Tumors

Sample	RQ of SEL1L mRNA	RQ of SEL1L protein	Sample	RQ of SEL1L mRNA	RQ of SEL1L protein
1	0.04	0.17	21[a]	0.49	0.81
2	0.04	0.36	22	0.52	0.67
3	0.04	0.09	23	0.54	1.25
4	0.04	0.13	24	0.58	0.57
5	0.06	0.38	25	0.76	1.42
6	0.07	0.09	26[a]	0.84	2.41
7	0.09	0.27	27	0.84	1.71
8	0.09	0.01	28	1.02	0.94
9[a]	0.11	1.09	29	1.02	0.68
10	0.12	0.28	30	1.05	1.70
11	0.13	0.33	31	1.14	1.89
12	0.15	0.16	32	1.14	1.20
13	0.16	0.14	33	1.25	1.27
14	0.24	0.35	34	1.38	0.57
15	0.29	0.39	35	1.40	1.39
16	0.35	0.20	36[a]	1.65	3.36
17[a]	0.38	1.18	37	1.85	1.44
18	0.39	0.47	38	2.74	4.10
19[a]	0.39	0.80	39[a]	2.81	1.66
20[a]	0.49	1.85	40	4.42	3.25

[a] *SEL1L* mRNA and SEL1L protein display different trends of expression.

A.

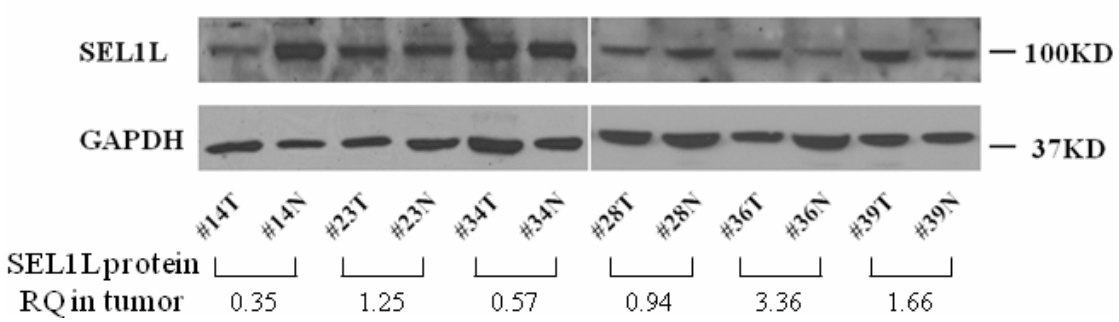

B.

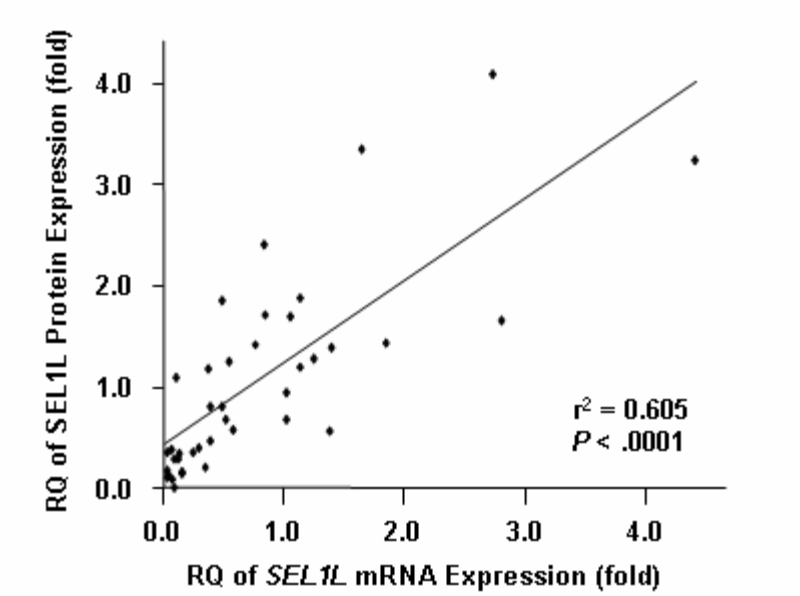

Figure 13. SEL1L protein expression and comparison to its mRNA expression.

A. Representative results of Western blotting (cropped image). Sample numbers follow table 5. T: PDAC tumor sample; N: normal adjacent tissue. **B.** Pearson's correlation scatter plot of SEL1L mRNA and protein relative fold change in 40 PDACs. The plot shows linear regression with $R^2 = 0.605$ (r = 0.778).

Expression of hsa-mir-143, hsa-mir-155, and hsa-mir-223 in pancreatic cancer cell lines were determined by qPCR

The hTERT-HPNE cell line was used as a "normal" control. This immortalized cell line was derived from normal ducts of the human pancreas and is the closest thing to normal human pancreas in terms of cell lines. The hTERT-HPNE cells have been found to have the ability to differentiate into pancreatic ductal cells [104].

The expression levels of hsa-mir-143, hsa-mir-155 and hsa-mir-223 were assessed in 12 pancreatic cancer cell lines and in the hTERT-HPNE cell line by qPCR. The RQs of these 3 miRNAs in the PDAC cell lines were then compared to the corresponding RQ in the hTERT-HPNE cell line. As shown in Figure 14, for hsa-mir-143, all the PDAC cell lines displayed relatively low levels of expression; for hsa-mir-155, the PDAC cell lines showed variable expression levels; for hsa-mir-223, only BxPC3 displayed a high level of expression and all of the other11 PDAC cell lines showed relatively low levels of expression.

The low expression level of hsa-mir-143 in the 12 PDAC cell lines indicates that these cell lines cannot serve as an ideal model for hsa-mir-143 functional analysis. Therefore, the functional analysis was focused on the other 2 miRNAs, hsa-mir-155 and hsa-mir-223.

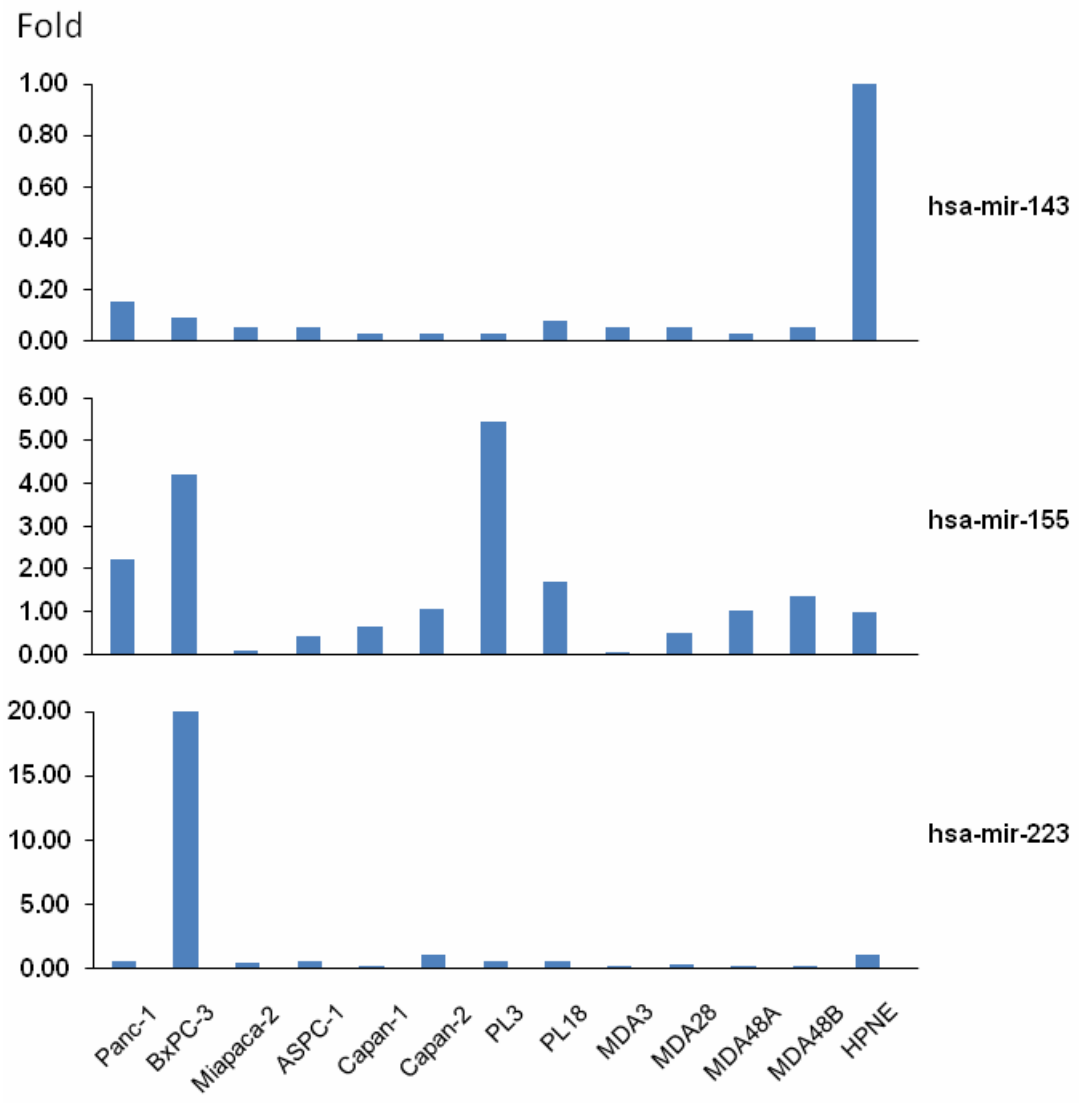

Figure 14. Expression of 3 miRNAs in PDAC cell lines.

Each column represents the relative expression level of the 3 miRNAs in the 12 PDAC cell lines. The expression level in the hTERT-HPNE cell line was set as 1 fold. Names of the miRNAs are labeled at the right, and names of the cell lines are labeled at the bottom.

pMIR-REPORT Luciferase Reporter construct vector showed decreased reporter expression in PL18 cell line

The pMIR-REPORT Luciferase Reporter Construct with putative hsa-mir-155 and hsa-mir-223 binding sites was transfected into two PDAC cell lines, PL18 and MDAPanc3, as described in the Methods. From the results in Figure 14, it was determined that PL18 has a relatively high expression level of hsa-mir-155; and MDAPanc3 has a very low expression level. Both of these 2 cell lines showed a low level of hsa-mir-223 expression. In the PL18 cells transfected with the construct vector, a significant decrease was found in firefly luciferase expression in comparison to the cells transfected with empty vector. However, for the MDAPanc3 cell line, there was no significant difference found in luciferase expression between the cells transfected with the construct vector and with the empty vector. These results are shown in Figure 15.

BxPC3 cells were also transfected with pMIR-REPORT Luciferase Reporter Vectors using the same protocol. It was determined that BxPC3 has a high expression level of both hsa-mir-155 and hsa-mir-223. However, there was no significant difference observed between the results of transfection of the construct vector and of the empty vector. It was noticed that the luciferase signal in BxPC3 cells was more than 100 times lower than that in other cells indicating low transfection efficiency in this cell line (data not shown). Therefore, the data obtained from experiments using BxPC3 cells may not be reliable.

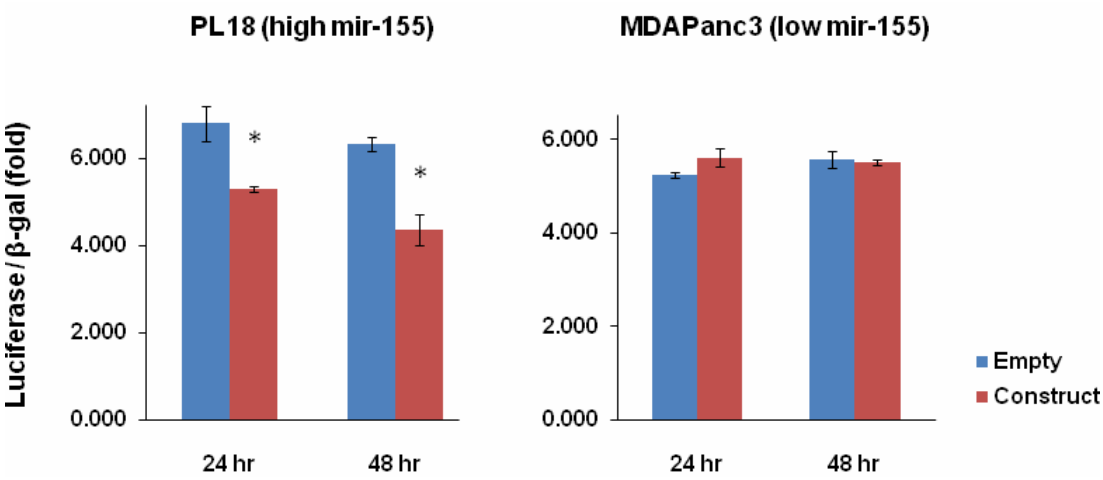

Figure 15. Luciferase assay of pMIR-REPORT Luciferase Reporter Vector transfection in 2 PDAC cell lines.

Empty: cells transfected with the vector without an insert. Construct: cells transfected with the vector containing the putative binding sites. The asterisk (*) indicates a significant difference between the results from empty vector transfection and the construct transfection (t-test, $P < 0.05$). Error bars indicate standard deviation of the relative luciferase expression (n = 3).

pMIR-REPORT Luciferase Reporter construct vector did not show difference in reporter expression in 293T cells co-transfected with the miRNA precursors

The 293T cell line is a derivative of HEK 293 cell lines containing the SV40 Large T-antigen. This cell line is easily transfected with plasmids containing the SV40 origin of replication. Gironella et al. used this cell line to co-transfect a reporter construct vector and hsa-mir-155 precusor [92]. Therefore, this cell line was chosen for the co-transfection experiment. However, there was no significant difference found in luciferase expression between the cells transfected with the negative control and with the miRNA precursors. Luciferase assay results from co-transfection of either the empty vector or the construct vector are shown in Figure 16.

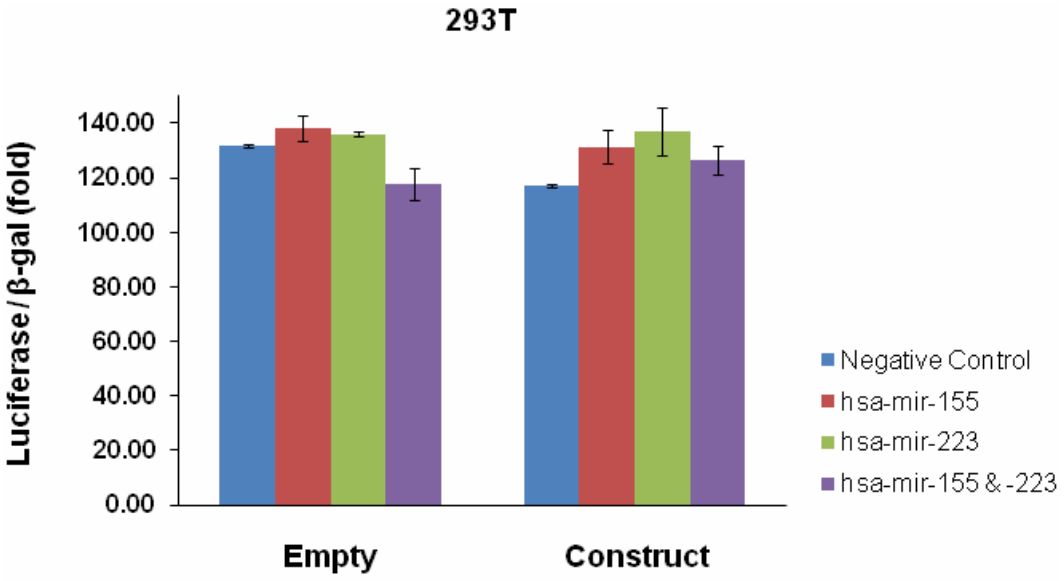

Figure 16. Luciferase assay of pMIR-REPORT Luciferase Reporter Vector co-transfection with miRNA precursors in 293T cell line.

Empty: cells transfected with the vector without an insert. Construct: cells transfected with the vector containing the putative binding sites. The cells were co-transfected with either the negative control, or 1 or 2 miRNA precursors. Error bars indicate standard deviation of the relative luciferase expression (n = 3).

SEL1L expression did not change after transfection of antagomirs

Because the BxPC3 cell line has very high expression levels of both hsa-mir-155 and hsa-mir-223, the antagomirs were transfected into this cell line to evaluate their effect on the expression of either one or two of the miRNAs. Real-time qPCR results indicated that 24 hours and 48 hours after transfection of the hsa-mir-155 antagomir, the expression of hsa-mir-155 was more than 2 fold downregulated. However, in the cells transfected with the hsa-mir-223 antagomir, there were no obvious changes in the expression of hsa-mir-223. Both qPCR and Western blotting did not reveal substantial changes in the expression of SEL1L at the mRNA level or protein level, including in the samples where hsa-mir-155 was downregulated. Results are shown in Figure 17.

The Capan2 cell line showed a moderate expression level of both hsa-mir-155 and hsa-mir-223. The antigomirs were transfected into this cell lines using the exact same protocol as for BxPC3. Similar results were obtained as seen for the BxPC3 cell line and the expression of SEL1L did not significantly change after the transfection of the antagomir(s). The results are shown in Figure 18.

The hsa-mir 155 antagomir was also been transfected into PL18 cells. This time, a double knockdown was performed as described in the Methods section. qPCR results indicated that hsa-mir-155 was further downregulated 48 hours after the second transfection (RQ = 0.18). However, there were still no substantial changes observed in the expression of SEL1L at either the mRNA level or protein level. The results are shown in Figure 19.

A.

Sample	Calibrator	mir155 RQ	mir223 RQ	SEL1L RQ
2. Anta 155 - 24 hr	1. NC - 24 hr	0.33	0.84	1.04
3. Anta 223 - 24 hr	1. NC - 24 hr	1.64	1.45	0.98
4. Anta 155+223 - 24 hr	1. NC - 24 hr	0.44	0.86	1.00
6. Anta 155 - 48 hr	5. NC - 48 hr	0.23	0.91	1.02
7. Anta 223 - 48 hr	5. NC - 48 hr	0.78	0.80	0.99
8. Anta 155+223 - 48 hr	5. NC - 48 hr	0.34	0.94	0.95

B.

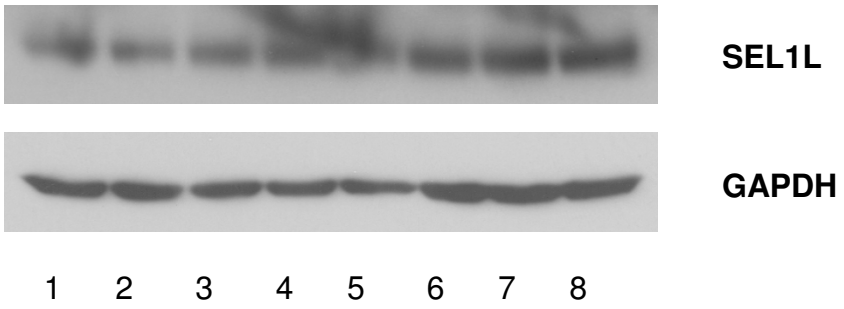

Figure 17. Expression of SEL1L after transfection of antagomirs against hsa-mir-155 and hsa-mir-223 in BxPC3 cells.

A. Relative quantities of hsa-mir-155, hsa-mir-223 and *SEL1L* mRNA determined by qPCR. Anta, samples transfected with antagomir(s); NC, samples transfected with negative control to antigomir; hr, hours after transfection. Sample numbers are noted at the left of each name. Red numbers indicate downregulation. **B.** SEL1L protein expression determined by Western blotting. Sample numbers are the same as those in panel A.

A.

Sample	Calibrator	SEL1L RQ
2. Anta 155 - 24hr	1. NC - 24 hr	1.05
3. Anta 223 - 24hr	1. NC - 24 hr	1.00
4. Anta 155+223 - 24hr	1. NC - 24 hr	1.03
6. Anta 155 - 48hr	5. NC - 48 hr	0.94
7. Anta 223 - 48hr	5. NC - 48 hr	0.97
8. Anta 155+223 - 48hr	5. NC - 48 hr	1.02

B.

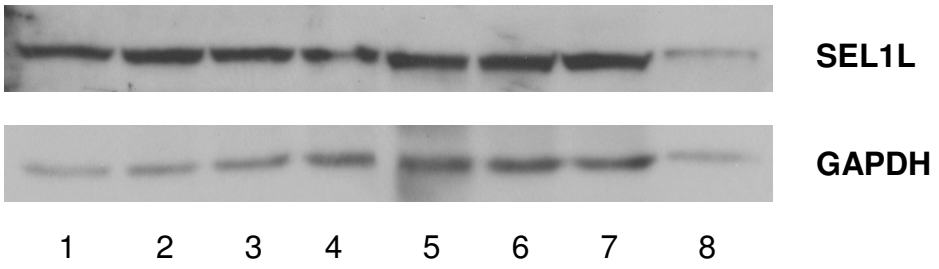

Figure 18. Expression of SEL1L after transfection of antagomirs against hsa-mir-155 and hsa-mir-223 in Capan2 cells.

A. Relative quantities of *SEL1L* mRNA determined by qPCR. Anta, samples transfected with antagomir(s); NC, samples transfected with negative control to antigomir; hr, hours after transfection. Sample numbers are noted at the left of each name. **B.** SEL1L protein expression determined by Western blotting. Sample numbers are the same as those in panel A.

A.

Sample	Calibrator	mir155 RQ	SEL1L RQ
2. Anta 155 - 24hr	1. NC - 24 hr	0.64	1.39
4. Anta 155 - 48hr	3. NC - 48 hr	0.40	1.03
6. Anta 155 - 72hr	5. NC - 72 hr	0.37	1.17
8. Double anta 155 - 24hr	7. Double NC - 24 hr	0.35	1.04
10. Double anta 155 - 48hr	9. Double NC - 48 hr	0.18	1.04

B.

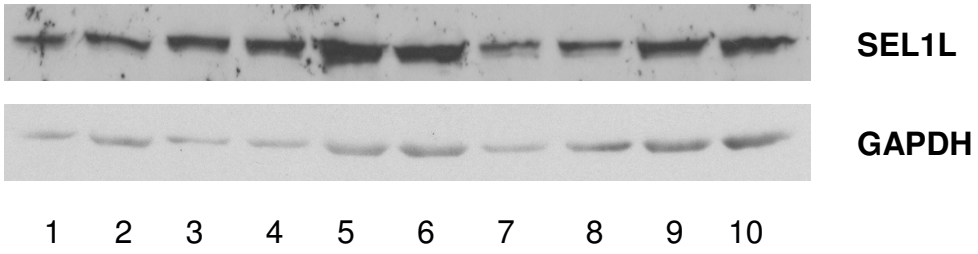

Figure 19. Expression of SEL1L after transfection of antagomir against hsa-mir-155 in PL18 cells.

A. Relative quantities of *SEL1L* mRNA determined by qPCR. Anta, samples transfected with antagomir; NC, samples transfected with negative control to antigomir; hr, hours after transfection. Double, transfection twice of the antagomir and the time points were taken after the second transfection. Sample numbers are noted at the left of each name. Red numbers indicate downregulation. **B.** SEL1L protein expression determined by Western blotting. Sample numbers are the same as those in panel A.

SEL1L protein expression was downregulated after transfection of hsa-mir-155 precursor in MDAPanc3 cells

Both MDAPanc3 and Miapaca2 cells have a very low expression level of hsa-mir-155 and hsa-mir-223. The expression levels of these 2 miRNAs were assessed after the transfection of the miRNA precursors using qPCR. As shown in Figure 20, the expression level of the miRNA markedly increased after transfection of the precursor when compared to the negative control (> 1000 folds). The endogenous control RNU6B exhibited similar expression levels for all the samples indicating that there was a similar amount of the initial cDNA.

The qPCR results in Figure 21A revealed that the expression level of SEL1L mRNA did not change even though hsa-mir-155 and hsa-mir-223 were overexpressed. However, from the Western blotting results in Figure 21B and 21C, it was determined that when hsa-mir-155 was overexpressed in MDAPanc3 cells the SEL1L protein displayed decreased expression level. When hsa-mir-223 alone was overexpressed, no significant changes were observed in SEL1L protein expression. When the precursors were transfected into Miapaca2 cells, there were no detectable changes in SEL1L expression levels (Figure 22).

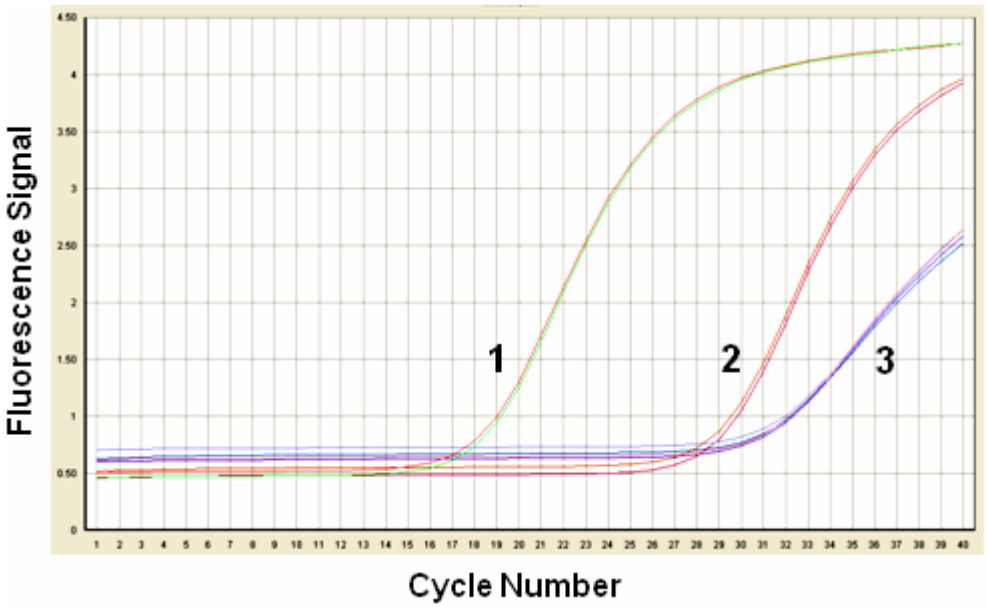

Figure 20. Representative qPCR amplification plot of miRNA expression after precursor transfection.

An increase in fluorescence indicates the detection of accumulated PCR product. Quantitation of the amount of target is measured by cycle number. The higher the initial amount of target cDNA, the sooner accumulated product is detected in the PCR process, and the lower the cycle number. Curve 1, detection of miRNA in sample transfected with miRNA precursor; curve 2, detection of miRNA in sample transfected with negative control to the precursor; curve 3, detection of RNU6B in both samples. All measurements were duplicated.

A.

Sample (MDAPanc3)	Calibrator (MDAPanc3)	SEL1L RQ
Pre 155 - 24hr	NC - 24 hr	1.56
Pre 223 - 24hr	NC - 24 hr	1.30
Pre 155+223 - 24hr	NC - 24 hr	0.96
Pre 155 - 48hr	NC - 48 hr	0.95
Pre 223 - 48hr	NC - 48 hr	1.00
Pre 155+223 - 48hr	NC - 48 hr	1.25
Pre 155 - 72hr	NC - 72 hr	1.09
Pre 223 - 72hr	NC - 72 hr	1.31
Pre 155+223 - 72hr	NC - 72 hr	1.12

B.

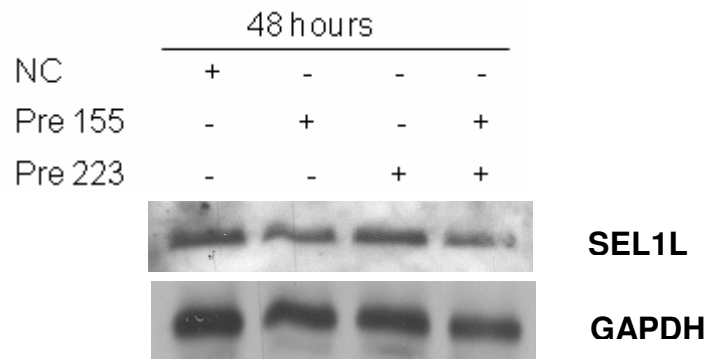

C.

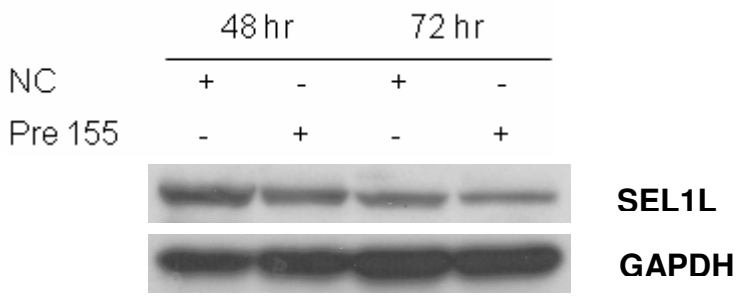

Figure 21. Expression of SEL1L after transfection of hsa-mir-155 and hsa-mir-223 precursors in MDAPanc3 cells.

A. Relative quantities of *SEL1L* mRNA determined by qPCR. Pre, samples transfected with miRNA precursor; NC, samples transfected with negative control to miRNA precursors; hr, hours after transfection. **B, C.** SEL1L protein expression determined by Western blotting.

A.

Sample (Miapaca2)	Calibrator (Miapaca2)	SEL1L RQ
Pre 155 - 24hr	NC - 24 hr	1.06
Pre 223 - 24hr	NC - 24 hr	1.27
Pre 155+223 - 24hr	NC - 24 hr	1.21
Pre 155 - 48hr	NC - 48 hr	1.47
Pre 223 - 48hr	NC - 48 hr	1.27
Pre 155+223 - 48hr	NC - 48 hr	1.20
Pre 155 - 72hr	NC - 72 hr	1.03
Pre 223 - 72hr	NC - 72 hr	0.64
Pre 155+223 - 72hr	NC - 72 hr	1.04

B.

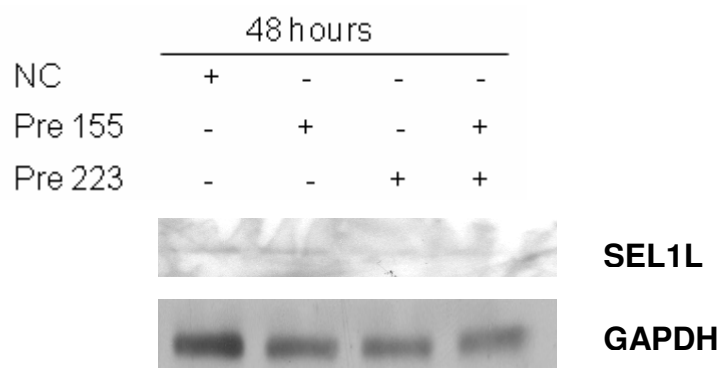

C.

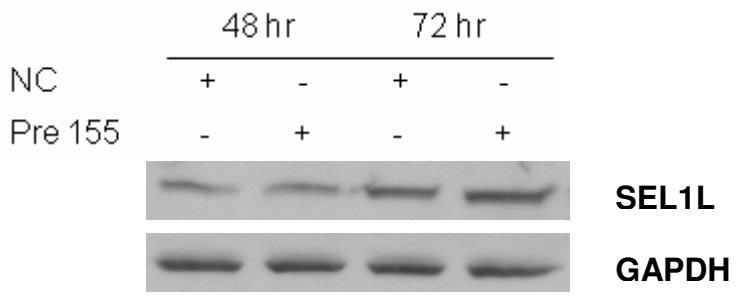

Figure 22. Expression of SEL1L after transfection of hsa-mir-155 and hsa-mir-223 precursors in Miapaca2 cells.

A. Relative quantities of *SEL1L* mRNA determined by qPCR. Pre, samples transfected with miRNA precursor; NC, samples transfected with negative control to miRNA precursors; hr, hours after transfection. **B, C.** SEL1L protein expression determined by Western blotting.

Sixteen proteins showed expression level changes after transfection of mir-155 precursor in MDAPanc3 cells

Reverse phase protein assay (RPPA) was applied to measure the transient response of the MDAPanc3 PDAC cells to the overexpression of hsa-mir-155. MDAPanc3 cells were transfected with hsa-mir-155 precursor or negative control and were collected after 48 hours and 72 hours, and then analyzed by RPPA. The expression levels of 12 proteins assessed were found to be downregulated and 4 were upregulated. Among these, 6 phosphorylation state-specific antibodies assessed phosphorylation at specific sites of target proteins. The relative quantities of these proteins are listed in Table 6A. All other proteins that were analyzed by RPPA did not show expression alterations and are listed in Table 6B. Through a search of the microRNA.org resource, it was determined that only the kinase insert domain receptor (*KDR*), epidermal growth factor receptor (*EGFR*), and v-rel reticuloendotheliosis viral oncogene homolog A (*RELA*) genes in Table 6Ahad potential binding sites to hsa-mir-155, therefore only these three genes would be expected to be downregulated by the overexpression of hsa-mir-155. This indicated that most of the protein expression changes were possibly induced through cellular networks instead of direct regulation by hsa-mir-155.

The data in Table 6A along with SEL1L protein expression data assessed by Western blotting were then uploaded to the IPA program. Through the use of IPA, 5 canonical pathways were found to be significantly associated with this data set, including pancreatic adenocarcinoma signaling and PTEN signaling (Table 7A). The three top involved networks were generated through the use of IPA and are

summarized in Table 7B. SEL1L was shown to be associated with a network which functions in cell death, gene expression and organismal development. Another downregulated protein, ERCC1, was shown to be in the same network.

Table 6. Protein Expression in Response to Hsa-mir-155 Overexpression in MDAPanc3 Cells Analyzed by RPPA

A. Proteins with Expression Alterations

Protein	Gene	48 hours	72 hours	Functions associated with cancer
Caveolin1	CAV1	0.609	0.511	tumor suppressor
Claudin7	CLDN7	0.489	1.014	tumor suppressor
HER2	ERBB2	0.643	0.913	onco-protein
HER2-pY1248	ERBB2	0.603	0.995	onco-protein
LKB1	STK11	0.634	0.911	tumor suppressor
Stat3_pS705	STAT3	0.619	0.962	transcription activator
KU80	XRCC5	0.664	1.018	DNA repair protein
ERCC1	ERCC1	0.614	1.043	DNA excision repair protein
VEGFR2	KDR	0.599	1.136	onco-protein
Tau	MAPT	0.590	1.258	stabilizing microtubules
Rad50	Rad50	0.625	1.066	DNA repair protein
EGFR	EGFR	0.863	0.658	onco-protein
NFkB_pS536	RELA	0.867	0.351	onco-protein
Beta Catenin	CTNNB1	1.710	1.538	onco-protein
YAP_pS127	YAP1	1.819	1.155	onco-protein
p38 MAPK-pT180/Y182	MAPK	1.524	1.224	transcription activator
p38 MAPK	CSBP	1.593	1.046	transcription activator
Shc-pY317	SHC1	1.089	1.516	regulating apoptosis

Yellow highlight: downregulation; blue highlight: upregulation

B. Proteins without Expression Alterations

Protein	48 hours	72 hours
ACC1	0.972	0.938
ACC_pS79	1.076	1.097
AIB1	1.213	0.941
AKT	1.054	0.930
AKT_pT308	1.238	1.355
Annexin	1.261	0.936
AR	1.088	1.002
ATM	0.844	0.950
Bak	0.997	0.984
BAX	1.390	0.931
Bcl2	0.937	1.145
BclX	0.929	0.845
BclxL	0.746	0.982
Beclin	1.166	1.053
BIM	1.063	0.873
cJun_pS73	0.909	1.294
cMet_pY1235	0.972	0.853
CadherinP	0.926	0.818
caspase3_active	0.914	0.857
Caspase7_cleaved	1.107	1.075
CDC2	0.970	1.045
CHK1	0.797	0.937
CHK1_pS345	1.089	1.289
CHK2_1C12	1.147	0.986
CHK2_pT68	1.060	0.904
cJun_pS73	1.016	1.272
CollagenVI	0.989	0.829
Cox2	1.115	0.988
CyclinB1	0.793	0.947
CyclinD1	0.757	1.032
CyclinE1	0.942	1.212
DJ1	1.319	0.933
E-cadherin	0.713	1.130
eEF2	1.205	0.953
eEF2K	0.903	0.757
EGFR_pY1173	1.076	1.072
eIF4E	1.079	0.997
Era	0.954	0.937
ERa_pS118	0.877	1.013
ERK2	1.312	1.339

Protein	48 hours	72 hours
FAK	0.877	1.212
FOX03a	1.147	0.869
FOX03a_pS318_321	0.896	1.203
FOXO3a_pS318	0.980	0.999
Gata3	1.121	0.953
GSK3beta	0.704	1.181
GSK3_pS21	0.953	1.000
IGFBP2	0.973	1.270
IGFR1b	0.935	0.881
INPP4B	0.908	0.993
IRS1	0.921	1.011
KitC	1.133	0.993
MAPK_pT202	1.457	0.999
MEK1	1.330	1.405
MEK1_pS217_221	1.096	0.917
Met	1.059	1.074
MIG6	0.886	0.835
Mre11_31H	0.894	0.913
MSH2	1.030	1.107
MSH6	0.684	1.119
mTOR	0.829	0.929
Myc	1.302	0.868
NF2	0.747	1.143
Notch1	0.975	0.855
Notch3	0.800	0.734
p21	0.894	0.937
p27	1.133	0.811
p27_pT157	0.976	0.877
p27_pT198	0.947	0.870
p53	0.721	1.098
p70S6K	0.946	0.919
p70S6K_pT389	1.187	1.326
p90RSK_pT359	0.700	0.947
p90RSK_pT359_S363	0.874	1.121
PARP_cleaved	0.845	1.229
Paxilline	1.167	1.179
PCNA	1.049	1.094
PDK1_pS241	1.432	1.327
Pea15	1.177	0.935

Protein	48 hours	72 hours
PI3K_p85	0.803	0.986
PI3K_p110a	1.301	0.936
PKC_pS657	1.017	1.059
PKCa	1.110	1.064
Pras40_pT246	0.992	0.928
PTCH	1.141	0.848
PTEN	1.053	1.344
Rab25	0.912	0.957
Rad51	0.939	0.989
RafB	1.085	1.359
RafC	1.227	1.224
RafC_pS338	0.954	0.985
Rb_pS807_811	0.816	0.859
Rb4H1	0.949	1.041
S6	0.831	1.016
S6_pS235_236	1.356	0.936
S6_pS240_244	0.766	0.936
Smad3	0.992	0.921
Smad4	0.751	0.906
Src	0.765	0.745
Src_pY416	1.120	0.958
Stat5	0.801	1.000
Stathmin	1.267	0.824
Taz	1.209	1.000
Taz_pS89	1.079	0.942
Transglutaminase	1.062	1.027
TSC2	0.919	1.046
Vasp	1.066	0.940
X4EBP1	1.285	0.942
X4EBP1_pS65	1.202	1.263
X4EBP1_pT37	1.430	1.050
X4EBP1_pT70	1.234	1.034
X53BP1	1.080	1.049
XBP1	0.996	0.954
Xiap	1.021	0.886
XRCC1	0.985	1.024
YAP	1.331	1.144
YB1	0.960	0.883
YB1_pS102	0.890	1.271

Table 7. Top Pathways and Networks Associated with the RPPA Data Sets Analyzed by IPA

A. Pathway	*P*-value	Genes Involved
Pancreatic Adenocarcinoma Signaling	3.14E-06	EGFR, ERBB2, RELA, STAT3
PTEN Signaling	3.26E-06	EGFR, KDR, RELA, SHC1
EGF Signaling	1.22E-05	EGFR, SHC1, STAT3
IL-15 Signaling	3.01E-05	RELA, SHC1, STAT3
PDGF Signaling	4.52E-05	CAV1, SHC1, STAT3

B. Top Network Associated Functions	Molecules in Network *
Cellular Development, Cancer, Cellular Growth and Proliferation	26s Proteasome, atypical protein kinase C, BCR, Calcineurin protein(s), Caspase, **CAV1, CLDN7,** Collagen Alpha1, Collagen type I, **ERBB2,** Estrogen Receptor, Focal adhesion kinase, **growth factor receptor,** Hsp27, Hsp70, Hsp90, Integrin, JAK, **KDR,** Laminin, **MAPT,** Mek, **NFkB (complex),** p85 (pik3r), Pdgf (complex), PDGF BB, Pdgfr, PLC gamma, PP2A, **RAD50, SHC1,** Sos, **STAT3,** Ubiquitin, **XRCC5**
Cancer, Gastrointestinal Disease, Organismal Injury and Abnormalities	14-3-3, Akt, Ap1, Calmodulin, Calpain, Cbp/p300, **CTNNB1, EGFR,** Endothelin, ERK, ERK1/2, Gsk3, Histone h3, IFN Beta, IgG, IL1, Insulin, Interferon alpha, Jnk, LDL, Mapk, NLRX1, **P38 MAPK,** PI3K (complex), Pka, Pkc(s), Ras, Ras homolog, **RELA,** Shc, SRC, STAT5a/b, **STK11,** Vegf, **YAP1**
Cell Death, Gene Expression and Organismal Development	CXCL12, dihydrotestosterone, EGF, **ERCC1,** ERCC5, FOS, HNF4A, HRAS, HSPA5, JUN, PTEN, RPA, **SEL1L,** SYVN1, TERF2, TFIIH, TNF, TNFRSF1A, TP53, tretinoin

* Molecules in network with bold font are genes in RPPA data set (plus SEL1L).

4.4 Discussion

In this study, aberrantly upregulated miRNAs in PDAC were studied to determine if they are involved in the downregulation of *SEL1L*. The miRNA target prediction tools helped in the selection of the miRNAs that potentially target *SEL1L*. However, the pairing match between a miRNA and a gene is not the only factor that influences the ability of a miRNA to bind and repress a target gene. Other characteristics, such as the binding position in the UTR, the flanking sequences, and mRNA secondary structures, are also important factors in predicting whether a miRNA is likely to repress the expression of a target gene [105]. Therefore, statistical methods were used to assess the probability that these 7 miRNAs target and repress *SEL1L* gene expression.

A significant correlation was observed between the expression of *SEL1L* mRNA and 3 of the 7 miRNAs that had potential binding sites for *SEL1L*. The expression of these 3 miRNAs (hsa-mir-143, hsa-mir-155, and hsa-mir-223) was found to be inversely associated with *SEL1L* mRNA expression in a high proportion of PDAC tumors, indicating that these miRNAs possibly repress the expression of *SEL1L* in some of the PDAC tumors.

Other investigators have shown that multiple coexpressed miRNAs can target a single mRNA and work together to repress the gene expression [106-108]. Velu et al. have recently demonstrated that two miRNAs, miR-21 and miR-196b, work synergistically in Lin^- bone marrow cells to increase the blocking of granulopoiesis [105]. Similarly, the data presented here demonstrated that the overexpression of an increasing number of functional miRNAs in PDAC is associated with an increasing

repression of *SEL1L* mRNA expression. This statistical result suggests that the 3 miRNAs may work cooperatively to regulate *SEL1L* expression.

Although hsa-mir-143, hsa-mir-155 and hsa-mir-223 are located on different chromosomes, a significant pairwise correlation between their expression profiles was observed. These results suggest that the deregulation of the 3 miRNAs may be caused by the same mechanism, such as mutant transcription factors that can bind to (or fail to bind to) the putative regulatory motifs that all 3 miRNA genes have in common [109]. Discovering and understanding the common regulatory mechanisms involved could provide new insight into the molecular mechanisms underlying pancreatic tumorigenesis.

A recent publication in *Nature* demonstrated that for miRNA regulatory interactions, more than 84% of the lowered protein production was associated with decreased mRNA levels [110]. The results indicated that destabilization of target mRNAs is the predominant impact of miRNAs on gene expression. In this study, the direct correlation between the expression of *SEL1L* mRNA and SEL1L protein also suggests that mRNA abundance is a key modulator for SEL1L protein expression in PDAC. For the small proportion of samples in which mRNA and protein expression were not correlated (20%), other mechanisms may be involved in regulation of SEL1L protein expression. Because many mechanisms affect protein levels at both the translational and the post-translational level, the disagreement in this small proportion of samples is not surprising [111].

Correlation between two variables does not imply that one directly causes the other, but it suggests a possible avenue warranting further investigation. In this study,

the statistical analysis results provided the rationale for conducting further *in vivo* functional analysis to explore the role of specific miRNAs in the regulation of SEL1L expression. Luciferease reporter assays, miRNA inhibition and overexpression experiments were performed to determine the relationship between SEL1L expression and the miRNAs from different aspects. Luciferase reporter assays are a method to determine if a miRNA truly binds to a predicted binding site in a gene. Through either miRNA inhibition or overexpression, it can be determined whether a miRNA causes a change in expression levels of a target gene.

It is hypothesized that in a cell line with high expression level of the miRNA, the reporter expression of vector containing the binding site would be repressed. In PL18 cells which have a relatively high expression level of hsa-mir-155, a significant decrease in luciferase expression was observed when comparing the experimental vector transfection to the results of empty vector transfection. There was no such decrease observed in MDAPanc3 cells which have a relatively low expression level of hsa-mir-155. These results suggest that hsa-mir-155 does bind to the predicted binding site in *SEL1L* gene. However, the possibility that this result reflected a difference between different cell lines cannot be ruled out.

Although BxPC3 has a high expression level of both hsa-mir-155 and hsa-mir-223, a decrease in luciferase expression was not detected when the cells were transfected with the experimental vector. This assay did not exhibit the expected result probably because of the low transfection efficiency in this cell line.

The cotransfection of luciferase vectors and miRNA precursors in 293T cells also did not show the expected results. One explanation for this result is that hsa-mir-

155 and hsa-mir-223 do not bind to the predicted binding sites. However, there are several possible reasons that may have caused a failure of this experiment. First, the miRNA precursors in this study do not contain a SV40 origin of replication; therefore, high transfection efficiency of the precusors would not be guaranteed, and it is possible that the plasmid and a precursor molecule were not transfected into the same cell. Second, after transfection a high rate of cell death was observed. The dead cells were removed after the PBS wash. The surviving cells examined by the luciferase assay may not be good representatives for the co-transfection.

For the miRNA knockdown experiments, it is hypothesized that inhibiting hsa-mir-155 and hsa-mir-223 would restore the expression of endogenous SEL1L. The qPCR results revealed that hsa-mir-155 was successfully downregulated by the antagomir, but the inhibition of hsa-mir-223 did not work for some unknown reason.

A significant increase in SEL1L expression was not detected at either the mRNA level or the protein level in the 3 PDAC cell lines, even though hsa-mir-155 was inhibited. Maybe hsa-mir-155 is not a modulator of SEL1L and this is the simplest explanation for these results. However, there are some other possibilities that should also be considered: (1) there is a delay of SEL1L expression change in response to the miRNA downregulation, and transient transfection may not reflect the delayed response; (2) the 2 to 4-fold reduction of hsa-mir-155 is not sufficient to cause a detectable change in SEL1L expression in these experiments; i.e. SEL1L expression might have been upregulated but it was not significant enough to be detected; (3) none of the 3 cell lines used in this study showed low expression of SEL1L and therefore, they may not serve as ideal models to use for examining regulation of *SEL1L* gene

expression. Another possibility is that more than one miRNA is required and this was not achieved under these experimental conditions.

When either hsa-mir-155 or hsa-mir-223 was overexpressed, it was hypothesized that the *SEL1L* gene would be downregulated. A decrease in expression of SEL1L protein was observed when the precursor of hsa-mir-155 was transfected in MDAPanc3 cells, either alone or with hsa-mir-223. When the precursor of hsa-mir-223 was transfected alone, a detectable downmodulation of SEL1L was not observed in either cell line. These results provided evidence that hsa-mir-155 is a suppressor of SEL1L, and hsa-mir-223 is not.

Unlike in PDAC tumors, in the cells where SEL1L protein expression was decreased there was no corresponding mRNA decrease. Larsson et al. found that transcripts with high turnover rates are less affected by miRNA overexpression after transfection [112]. This may be the explanation for the results that SEL1L mRNA perhaps has a high turnover rate and the expression level of the mRNA was not significantly affected by the transient transfection of hsa-mir-155.

MDAPanc3 cell line was established in my adviser (Dr. Frazier)'s laboratory, from a liver metastasis of PDAC [113], whereas Miapaca2 was derived from a grade G3 primary PDAC tumor [114]. Using Spectral Karyotyping, Sirivatanauksorn et al showed that these two cell lines had different cytogenetic aberrations [115]. Because of the different histological and genetic background, it is not a surprise that the results from these two cell lines are different. The interaction between hsa-mir-155 and SEL1L might be interrupted in Miapaca2 cells by unknown factors not found in MDAPanc3. Another possibility is that the interaction reflects an indirect interaction

in which the overexpressed hsa-mir-155 regulated SEL1L expression through certain signaling pathways in MDAPanc3 cells, and these pathways might be disrupted in Miapaca2 cells.

In conclusion, the functional analysis revealed that in the tested PDAC cell lines hsa-mir-223 did not act as a suppressor of SEL1L; hsa-mir-155 acted as a suppressor of SEL1L but only under some cellular environments, which could be the specific genetic background of the cell lines.

Hsa-miR-155 has been reported to be involved in various biological processes, such as haematopoiesis, inflammation and immunity. It plays an oncogenic role in the pathogenesis of numerous cancers, including leukemia, breast cancer, colon cancer, lung cancer, and PDAC [116, 117]. Dr. Sen's group found elevated expression levels of hsa-mir-155 in the plasma of PDAC patients as compared with plasma from healthy controls, suggesting that this miRNA may serve as a blood-based biomarker for the detection of PDAC [118]. This miRNA has also been reported as a biomarker of early pancreatic neoplasia [119].

In this study, using RPPA and IPA the evidence suggested that hsa-mir-155 may impact the progression of PDAC not only through direct regulation of target genes, but also through a series of pathways and networks. Interestingly, several very important signaling pathways in PDAC were shown to be influenced by hsa-mir-155 modulation in PDAC cell lines. Due to the limited number of validated antibodies in the RPPA experiment, not all genes that were affected by the upregulation of this miRNA could be detected. To validate the RPPA data, the variations of the protein expression need to be confirmed by Western blotting in future studies.

In conclusion, this study combined statistical analysis with biological approaches to determine the relationships between several miRNAs and the *SEL1L* gene. The finding that the expression of tumor suppressor *SEL1L* was repressed by the upregulation of hsa-mir-155 elucidated the mechanism for *SEL1L* downregulation in some PDAC cases. The findings provided evidence for using miRNAs as new approaches for the detection, prevention and treatment of this dismal disease.

SUMMARY AND FUTURE DIRECTIONS

In this study, the aberrations of the putative tumor suppressor gene *SEL1L* in PDAC tumors were investigated. The goal was to determine the mechanism(s) of *SEL1L* downregulation. *SEL1L* downregulation was confirmed in a significant proportion of the tumors at both mRNA level and protein level. For the first time, abundant presence of variant splicing products of *SEL1L* were observed in PDAC, and for the first time LOH was detected in the *SEL1L* gene in 15.4% of the tumors. It was determined that mutations, LOH and promoter methylation are not the mechanisms of SEL1L downregulation. Data was generated demonstrating that overexpression of hsa-mir-155 may cause *SEL1L* downregulation in some PDAC cases. It is possible that some other miRNAs that were not included in this study may target and repress *SEL1L* expression. No mutations were detected in the *SEL1L* coding region. As tumor suppressor genes generally follow the "two-hit hypothesis" [120], which implies that cancer is the result of accumulated mutations to a cell's DNA, although *SEL1L* has functions involving tumor suppression it cannot be identified as a classical tumor suppressor gene.

The findings of the studies described in this thesis provide a better understanding of the abnormalities of the *SEL1L* gene in PDAC, which could lead to new approaches for the early detection, prevention and treatment of this dismal disease. Through these studies, besides having learned new techniques, I have expanded my knowledge and experience in problem solving, critical thinking and data analysis, as well as connecting laboratory findings to clinical information. However,

there are still many questions that remain as a result of my studies that lead to future studies.

For the finding of variant splicing products of *SEL1L*, at this point it is not clear if these products are specifically associated with PDAC tumors since they were also observed in normal-appearing adjacent tissues. However, normal appearing tissue adjacent to the cancer in general is not normal even though the histological appearance may be normal. The "normal" tissues may display biomarkers that are found in the tumor due to underlying genetic events that they share with the tumor, but do not display all of the molecular features that the cancer has. This is called a field effect and has recently been reviewed by Chai and Brown [121]. As discussed in Chapter 1, to determine whether there are tumor-specific *SEL1L* transcripts in PDAC, further tests with microdissected tissues and deep sequencing are necessary. As mentioned above in Chapter 1, mis-splicing similar to what we have observed has been reported for other genes. So far, there is no reported explanation for this mis-splicing phenomenon. Future studies could examine several PDAC cell lines using RT-PCR and subcloning to see whether variant transcripts of SEL1L mRNA can be detected. This might allow us to determine if the variant transcripts arise clonally. If higher frequency of variant transcripts is observed in the PDAC cells than in the HPNE cells, DNA microarray could be performed to determine whether there are expression alterations in splicing machinery-related genes in the PDAC cells when compared to HPNE cells. If altered splicing machinery-related genes are identified, the next step would be to restore the normal expression of the gene and determine whether SEL1L splicing becomes normal.

In this study, it was determined that overexpression of hsa-mir-155 may be one of the factors that repress SEL1L expression, but it does not explain the abnormal expression of SEL1L in all of the PDAC samples. During the past several years, the miRNA databases have been expanding and many newly discovered miRNAs were not included in this study. Therefore it is possible that there are other miRNAs regulating SEL1L expression that we did not test. Also there are some other mechanisms of gene downregulation that were not studied. These should be investigated in the future, such as histone modification [122, 123] and pseudogene silencing [124-126].

Another path of investigation of the *SEL1L* gene that might shed light on its role in pancreatic cancer is its association with other known signaling pathways. Overexpression of *SEL1L* in human PDAC cells increased the expression levels of Smad4, activin A, TIMP and PTEN, suggesting an interaction of SEL1L with the TGFβ and PTEN signaling pathways [30, 33]. The RPPA data presented in this thesis and IPA analysis indicate a possible interaction of SEL1L with the proteins in the "cell death, gene expression, organismal development" network. However, the RPPA results still need to be confirmed by Western analysis, and the most informative approach to pursue the elaboration of pathways that are influenced by SEL1L would be to develop a pancreas-specific knock-out mouse model. Using this kind of model, it would be possible to determine whether the mice develop pancreatic cancer, and whether the reported signaling pathways and networks are truly influenced. Some physiological conditions, such as glucose starvation or hypoxia, may need to be applied for the activation of the UPR/ERAD pathway. Since there are two distinct

directions of the UPR/ERAD pathway, the stimulation of this pathway should be quantitatively adjusted to control the amount of generated unfolded/misfolded proteins.

Hopefully on the basis of the studies described in this thesis, future studies will build upon these findings in order to understand the pathogenesis of PDAC, and the further characterization of biomarkers for early detection and prevention of PDAC. This will put us one step closer to defeating this devastating disease.

REFERENCES

[1] Pancreas. Wikipedia, the free encyclopedia. Retrieved, January 24, 2011, from: http://en.wikipedia.org/wiki/Pancreas

[2] Jemal A, Siegel R, Xu J, Ward E. Cancer Statistics, 2010. CA Cancer J Clin 2010; 60: 277-300.

[3] American Cancer Society. Cancer Facts & Figures 2010. Atlanta: American Cancer Society; 2010.

[4] Types of Pancreas Tumors. Johns Hopkins University, The Sol Goldman Pancreatic Cancer Research Center. Retrieved, January 24, 2011, from http://pathology.jhu.edu/pancreas/BasicTypes1.php

[5] Hruban RH, Fukushima N. Pancreatic adenocarcinoma: update on the surgical pathology of carcinomas of ductal origin and PanINs. Mod Pathol 2007; 20 Suppl 1: S61-70.

[6] Parsa I, Longnecker DS, Scarpelli DG, Pour P, Reddy JK, Lefkowitz M. Ductal metaplasia of human exocrine pancreas and its association with carcinoma. Cancer Res 1985; 45: 1285-1290.

[7] Hruban RH, Wilentz RE, Goggins M, Offerhaus GJ, Yeo CJ, Kern SE. Pathology of incipient pancreatic cancer. Ann Oncol 1999; 10: 9-11.

[8] Hruban RH, Adsay NV, Albores-Saavedra J, Compton C, Garrett ES, Goodman SN, Kern SE, Klimstra DS, Klöppel G, Longnecker DS, Lüttges J, Offerhaus GJ. Pancreatic intraepithelial neoplasia: a new nomenclature and classification system for pancreatic duct lesions. Am J Surg Pathol 2001; 25: 579-586.

[9] Guerra C, Schuhmacher AJ, Canamero M, Grippo PJ, Verdaguer L, Perez-Gallego L, Dubus P, Sandgren EP, Barbacid M. Chronic pancreatitis is essential for induction of pancreatic ductal adenocarcinoma by K-Ras oncogenes in adult mice. Cancer Cell 2007; 11: 291-302.

[10] Habbe N, Shi G, Meguid RA, Fendrich V, Esni F, Chen H, Feldmann G, Stoffers DA, Konieczny SF, Leach SD, Maitra A. Spontaneous induction of murine pancreatic intraepithelial neoplasia (mPanIN) by acinar cell targeting of oncogenic Kras in adult mice. Proc Natl Acad Sci U S A 2008; 105: 18913-18918.

[11] Means AL, Meszoely IM, Suzuki K, Miyamoto Y, Rustgi AK, Coffey RJ Jr, Wright CV, Stoffers DA, Leach SD. Pancreatic epithelial plasticity mediated by acinar cell transdifferentiation and generation of nestin-positive intermediates. Development 2005; 132: 3767-3776.

[12] Hahn SA, Seymour AB, Hoque AT, Schutte M, Costa LT, Redston MS, Caldas C, Weinstein CL, Fischer A, Yeo CJ, Hruban RH, Kern SE. Allelotype of pancreatic adenocarcinoma using xenograft enrichment. Cancer Rec 1995; 55: 4670-4675.

[13] Luttges J, Galehdari H, Brocker V, Schwarte-Waldhoff I, Henne-Bruns D, Kloppel G, Schmiegel W, Hahn SA. Allelic loss is often the first hit in the biallelic inactivation of the p53 and DPC4 genes during pancreatic carcinogenesis. Am J Pathol 2001; 158: 1677-1683.

[14] Imai M, Nakamura T, Akiyama T, Horii A. Infrequent somatic mutations of the *ICAT* gene in various human cancers with frequent 1p-LOH and/or abnormal nuclear accumulation of β-catenin. Oncol Rep 2004; 12: 1099-1103.

[15] Kimura M, Abe T, Sunamura M, Matsuno S, Horii A. Detailed deletion mapping on chromosome arm 12q in human pancreatic adenocarcinoma: identification of a 1-cM region of common allelic loss. Genes Chromosomes Cancer 1996; 17: 88-93.

[16] Kimura M, Furukawa T, Abe T, Yatsuoka T, Youssef EM, Yokoyama T, Ouyang H, Ohnishi Y, Sunamura M, Kobari M, Matsuno S, Horii A. Identification of two common regions of allelic loss in chromosome arm 12q in human pancreatic cancer. Cancer Res 1998; 58: 2456-2460.

[17] Fukushige S, Furukawa T, Satoh K, Sunamura M, Kobari M, Koizumi M, Horii A. Loss of chromosome 18q is an early event in pancreatic ductal tumors. Cancer Res 1998; 58: 4222-4226.

[18] Fukushige S, Waldman FM, Kimura M, Abe T, Furukawa T, Sunamura M, Kobari M, Horii A. Frequent gain of copy number on the long arm of chromosome 20 in human pancreatic adenocarcinoma. Genes Chromosomes Cancer 1997; 19: 161-169.

[19] Hruban RH, Goggins M, Parsons J, Kern SE. Progression model for pancreatic cancer. Clin Cancer Res 2000; 6: 2969-2972.

[20] Bardeesy N, Depinho RA. Pancreatic cancer biology and genetics. Nat Rev Cancer 2002; 2: 897-909.

[21] Moskaluk CA, Hruban RH, Kern SE. p16 and K-ras gene mutations in the intraductal precursors of human pancreatic adenocarcinoma. Cancer Res 1997; 57: 2140-2143.

[22] Berman DM, Karhadkar SS, Maitra A, Montes De Oca R, Gerstenblith MR, Briggs K, Parker AR, Shimada Y, Eshleman JR, Watkins DN, Beachy PA.

Widespread requirement for Hedgehog ligand stimulation in growth of digestive tract tumours. Nature 2003; 425: 846-851.

[23] Thayer SP, Di Magliano MP, Heiser PW, Nielsen CM, Roberts DJ, Lauwers GY, Qi YP, Gysin S, Fernández-del Castillo C, Yajnik V, Antoniu B, McMahon M, Warshaw AL, Hebrok M. Hedgehog is an early and late mediator of pancreatic cancer tumorigenesis. Nature 2003; 425: 851-856.

[24] Kayed H, Kleeff J, Keleg S, Guo J, Ketterer K, Berberat PO, Giese N, Esposito I, Giese T, Büchler MW, Friess H. Indian hedgehog signaling pathway: expression and regulation in pancreatic cancer. Int J Cancer 2004; 110: 668-676.

[25] Sen S, Zhou H, White RA. A putative serine/threonine kinase encoding gene BTAK on chromosome 20q13 is amplified and over-expressed in human breast cancer cell lines. Oncogene 1997; 14: 2195-2200.

[26] Li D, Zhu J, Firozi PF, Abbruzzese JL, Evans DB, Cleary K, Friess H, Sen S. Overexpression of oncogenic STK15/BTAK/Aurora A kinase in human pancreatic cancer. Clin Cancer Res 2003; 9: 991-997.

[27] Morris JP 4th, Wang SC, Hebrok M. KRAS, Hedgehog, Wnt and the twisted developmental biology of pancreatic ductal adenocarcinoma. Nat Rev Cancer 2010; 10: 683-695.

[28] Balasenthil S, Chen N, Lott ST, Chen J, Carter J, Grizzle WE, Frazier ML, Sen S, Killary AM. A migration signature and plasma biomarker panel for pancreatic adenocarcinoma. Cancer Prev Res (Phila) 2011; 4: 137-149.

[29] Biunno I, Appierto V, Cattaneo M, Leone BE, Balzano G, Socci C, Saccone S, Letizia A, Della Valle G, Sgaramella V. Isolation of a pancreas-specific gene located

on human chromosome 14q31: expression analysis in human pancreatic ductal carcinomas. Genomics 1997; 46: 284-286.

[30] Harada Y, Ozaki K, Suzuki M, Fujiwara T, Takahashi E, Nakamura Y, Tanigami A. Complete cDNA sequence and genomic organization of a human pancreas-specific gene homologous to Caenorhabditis elegans sel-1. J Hum Genet 1999; 44: 330-336.

[31] Cattaneo M, Orlandini S, Beghelli S, Moore PS, Sorio C, Bonora A, Bassi C, Talamini G, Zamboni G, Orlandi R, Ménard S, Bernardi LR, Biunno I, Scarpa A. SEL1L expression in pancreatic adenocarcinoma parallels SMAD4 expression and delays tumor growth in vitro and in vivo. Oncogene 2003; 22: 6359-6368.

[32] Grant B, Greenwald I. The Caenorhabditis elegans sel-1 gene, a negative regulator of lin-12 and glp-1, encodes a predicted extracellular protein. Genetics 1996; 143: 237-247.

[33] Grant B, Greenwald I. Structure, function, and expression of SEL-1, a negative regulator of LIN-12 and GLP-1 in C. elegans. Development 1997; 124: 637-644.

[34] Cattaneo M, Fontanella E, Canton C, Delia D, Biunno I. SEL1L affects human pancreatic cancer cell cycle and invasiveness through modulation of PTEN and genes related to cell-matrix interactions. Neoplasia 2005; 7: 1030-1038.

[35] Thierry-Mieg D, Thierry-Mieg J. AceView: a comprehensive cDNA-supported gene and transcripts annotation. Genome Biol 2006; 7: S12.1-14.

[36] Hampton RY, Gardner RG, Rine J. Role of 26S proteasome and HRD genes in the degradation of 3-hydroxy-3-methylglutaryl-CoA reductase, an integral endoplasmic reticulum membrane protein. Mol Biol Cell 1996; 7: 2029-2044.

[37] Gardner RG, Swarbrick GM, Bays NW, Cronin SR, Wilhovsky S, Seelig L, Kim C, Hampton RY. Endoplasmic reticulum degradation requires lumen to cytosol signaling. Transmembrane control of Hrd1p by Hrd3p. J Cell Biol 2000; 151: 69-82.

[38] Cattaneo M, Canton C, Albertini A, Biunno I. Identification of a region within SEL1L protein required for tumour growth inhibition. Gene 2004; 326: 149-156.

[39] Kaneko M, Nomura Y. ER signaling in unfolded protein response. Life Sci 2003; 74: 199-205.

[40] Mueller B, Lilley BN, Ploegh HL. SEL1L, the homologue of yeast Hrd3p, is involved in protein dislocation from the mammalian ER. J Cell Biol 2006; 175: 261-270.

[41] Endoplasmic reticulum. Wikipedia, the free encyclopedia**.** Retrieved, January 24, 2011, from: http://en.wikipedia.org/wiki/Endoplasmic_reticulum

[42] Kaufman RJ. Stress signaling from the lumen of the endoplasmic reticulum: coordination of gene transcriptional and translational controls. Genes Dev 1999; 13: 1211-1233.

[43] Kozutsumi Y, Segal M, Normington K, Gething MJ, Sambrook J. The presence of malfolded proteins in the endoplasmic reticulum signals the induction of glucose-regulated proteins. Nature 1988; 332: 462-464.

[44] Dorner AJ, Wasley LC, Kaufman RJ. Increased synthesis of secreted proteins induces expression of glucose-regulated proteins in butyrate-treated Chinese hamster ovary cells. J Biol Chem 1989; 264: 20602-20607.

[45] Hu P, Han Z, Couvillon AD, Exton JH. Critical role of endogenous Akt/IAPs and MEK1/ERK pathways in counteracting endoplasmic reticulum stress-induced cell death. J Biol Chem 2004; 279: 49420-49429.

[46] Kane LP, Shapiro VS, Stokoe D, Weiss A. Induction of NF-kappaB by the Akt/PKB kinase. Curr Biol 1999; 9: 601-604.

[47] Sonenshein GE. Rel/NF-kappa B transcription factors and the control of apoptosis. Semin Cancer Biol 1997; 8: 113-119.

[48] Herrmann JL, Bruckheimer E, McDonnell TJ. Cell death signal transduction and Bcl-2 function. Biochem Soc Trans 1996; 24: 1059-1065.

[49] Ahmed NN, Grimes HL, Bellacosa A, Chan TO, Tsichlis PN. Transduction of interleukin-2 antiapoptotic and proliferative signals via Akt protein kinase. Proc Natl Acad Sci U S A 1997; 94: 3627-3632.

[50] Lawson B, Brewer JW, Hendershot LM. Geldanamycin, an hsp90/GRP94-binding drug, induces increased transcription of endoplasmic reticulum (ER) chaperones via the ER stress pathway. J Cell Physiol 1998; 174: 170-178.

[51] Hitomi J, Katayama T, Eguchi Y, Kudo T, Taniguchi M, Koyama Y, Manabe T, Yamagishi S, Bando Y, Imaizumi K, Tsujimoto Y, Tohyama M. Involvement of caspase-4 in endoplasmic reticulum stress-induced apoptosis and Abeta-induced cell death. J Cell Biol 2004; 165: 347-356.

[52] Diaferia G, Cattaneo M, Saltini G, Proverbio MC, Monferini E, Malferrari G, Albertini A, Biunno I. RNA-mediated interference indicates that SEL1L plays a role in pancreatic beta-cell growth. DNA Cell Biol 2004; 23: 510-518.

[53] Altschul SF, Gish W, Miller W, Myers EW, Lipman DJ. Basic local alignment search tool. J Mol Biol 1990; 215: 403-410.

[54] Lee MP, Feinberg AP. Aberrant splicing but not mutations of TSG101 in human breast cancer. Cancer Res 1997; 57: 3131-3134.

[55] Oh Y, Proctor ML, Fan YH, Hong WK, Fong KM, Sekido YS, Gazdar AF, Minna JD, Mao L. TSG101 is not mutated in lung cancer but a shortened transcript is frequently expressed in small cell lung cancer. Oncogene 1998; 17: 1141-1148.

[56] Sigalas I, Calvert AH, Anderson JJ, Neal DE, Lunec J. Alternatively spliced mdm2 transcripts with loss of p53 binding domain sequences: transforming ability and frequent detection in human cancer. Nat Med 1996; 2: 912-917.

[57] Matsumoto R, Tada M, Nozaki M, Zhang CL, Sawamura Y, Abe H. Short alternative splice transcripts of the mdm2 oncogene correlate to malignancy in human astrocytic neoplasms. Cancer Res 1998; 58: 609-613.

[58] Lukas J, Gao DQ, Keshmeshian M, Wen WH, Tsao-Wei D, Rosenberg S, Press MF. Alternative and aberrant messenger RNA splicing of the mdm2 oncogene in invasive breast cancer. Cancer Res 2001; 61: 3212-3219.

[59] Negrini M, Monaco C, Vorechovsky I, Ohta M, Druck T, Baffa R, Huebner K, Croce CM. The *FHIT* gene at 3p14.2 is abnormal in breast carcinomas. Cancer Res 1996; 56: 3173-3179.

[60] Virgilio L, Shuster M, Gollin S, Veronese ML, Ohta M, Huebner K, Croce CM. *FHIT* gene alterations in head and neck squamous cell carcinomas. Proc Natl Acad Sci USA 1996; 93: 9770-9775.

[61] Fong K, Biesterveld E, Virmani A, Wistuba I, Sekido Y, Bader SA, Ahmadian M, Ong ST, Rassool FV, Zimmerman PV, Giaccone G, Gazdar AF, Minna JD. FHIT and FRA3B 3p14.2 allele loss are common in lung cancer and preneoplastic bronchial lesions are associated with cancer-related FHIT cDNA splicing aberrations. Cancer Res 1997; 57: 2256-2267.

[62] Ding WQ, Kuntz SM, Miller LJ. A misspliced form of the cholecystokinin-B/gastrin receptor in pancreatic carcinoma: role of reduced sellular U2AF35 and a suboptimal 3'-splicing site leading to retention of the fourth intron. Cancer Res 2002; 62: 947-952.

[63] Choudhury A, Moniaux N, Winpenny JP, Hollingsworth MA, Aubert JP, Batra SK. Human MUC4 mucin cDNA and its variants in pancreatic carcinoma. J Biochem 2000; 128: 233-243.

[64] Hayes GM, Carrigan PE, Miller LJ. Serine-arginine protein kinase 1 overexpression is associated with tumorigenic imbalance in mitogen-activated protein kinase pathways in breast, colonic, and pancreatic carcinomas. Cancer Res 2007; 67: 2072-2080.

[65] Kaufmann D, Leistner W, Kruse P, Kenner O, Hoffmeyer S, Hein C, Vogel W, Messiaen L, Bartelt B. Aberrant splicing in several human tumors in the tumor suppressor genes neurofibromatosis type 1, neurofibromatosis type 2, and tuberous sclerosis 2. Cancer Res 2002; 62: 1503-1509.

[66] Klinck R, Bramard A, Inkel L, Dufresne-Martin G, Gervais-Bird J, Madden R, Paquet ER, Koh C, Venables JP, Prinos P, Jilaveanu-Pelmus M, Wellinger R,

Rancourt C, Chabot B, Abou Elela S. Multiple alternative splicing markers for ovarian cancer. Cancer Res 2008; 68: 657-663.

[67] Venables JP, Klinck R, Bramard A, Inkel L, Dufresne-Martin G, Koh C, Gervais-Bird J, Lapointe E, Froehlich U, Durand M, Gendron D, Brosseau JP, Thibault P, Lucier JF, Tremblay K, Prinos P, Wellinger RJ, Chabot B, Rancourt C, Elela SA. Identification of alternative splicing markers for breast cancer. Cancer Res 2008; 68: 9525-9531.

[68] Cavenee W,,Dryja TP, Phillips RA, Benedict WF, Godbout R, Gallie BL, Murphree AL, Strong LC, White R. Expression of recessive alleles by chromosomal mechanisms in retinoblastoma. Nature 1983; 305: 779-784.

[69] Seymour AB, Hruban RH, Redston M, Caldas C, Powell SM, Kinzler KW, Yeo CJ, Kern SE. Allelotype of pancreatic adenocarcinoma. Cancer Res 1994; 54: 2761-2764.

[70] Chiaramonte R, Sabbadini M, Balordi F, Comi P, Sherbet GV. Allele frequency of two intragenic microsatellite loci of SEL1L gene in Northern Italian population. Mol Cell Biochem 2002; 232: 159-161.

[71] Livak KJ, Schmittgen TD. Analysis of relative gene expression data using real-time quantitative PCR and the 2(-Delta Delta C(T)) method. Methods 2001; 25: 402-408.

[72] Canzian F, Salovaara R, Hemminki A, Kristo P, Chadwick RB, Aaltonen LA, de la Chapelle A. Semiautomated assessment of loss of heterozygosity and replication error in tumors. Cancer Res 1996; 56: 3331-3337.

[73] Jones PA, Takai D. The role of DNA methylation in mammalian epigenetics. Science 2001; 293: 1068-1070.

[74] Li E. Chromatin modification and epigenetic reprogramming in mammalian development. Nature Rev Genet 2002; 3: 662–673.

[75] Esteller M. CpG island hypermethylation and tumor suppressor genes: a booming present, a brighter future. Oncogene 2002; 21: 5427-5440.

[76] Nakata S, Sugio K, Uramoto H, Oyama T, Hanagiri T, Morita M, Yasumoto K. The methylation status and protein expression of CDH1, p16(INK4A), and fragile histidine triad in nonsmall cell lung carcinoma: epigenetic silencing, clinical features, and prognostic significance. Cancer 2006; 106: 2190-2199.

[77] Nosho K, Yamamoto H, Takahashi T, Mikami M, Taniguchi H, Miyamoto N, Adachi Y, Arimura Y, Itoh F, Imai K, Shinomura Y. Genetic and epigenetic profiling in early colorectal tumors and prediction of invasive potential in pT1 (early invasive) colorectal cancers. Carcinogenesis 2007; 28: 1364-1370.

[78] Oue N, Oshimo Y, Nakayama H, Ito R, Yoshida K, Matsusaki K, Yasui W. DNA methylation of multiple genes in gastric carcinoma: association with histological type and CpG island methylator phenotype. Cancer Sci 2003; 94: 901-905.

[79] Hesson L, Bièche I, Krex D, Criniere E, Hoang-Xuan K, Maher ER, Latif F. Frequent epigenetic inactivation of RASSF1A and BLU genes located within the critical 3p21.3 region in gliomas. Oncogene 2004; 23: 2408-2419.

[80] Kim DH, Kim JS, Park JH, Lee SK, Ji YI, Kwon YM, Shim YM, Han J, Park J. Relationship of Ras association domain family 1 methylation and K-ras mutation in primary non-small cell lung cancer. Cancer Res 2003; 63: 6206-6211.

[81] Teodoridis JM, Hall J, Marsh S, Kannall HD, Smyth C, Curto J, Siddiqui N, Gabra H, McLeod HL, Strathdee G, Brown R. CpG island methylation of DNA damage response genes in advanced ovarian cancer. Cancer Res 2005; 65: 8961-8967.

[82] Hanabata T, Tsukuda K, Toyooka S, Yano M, Aoe M, Nagahiro I, Sano Y, Date H, Shimizu N. DNA methylation of multiple genes and clinicopathological relationship of non-small cell lung cancers. Oncol Rep 2004; 12: 177-180.

[83] Ogino S, Kawasaki T, Kirkner GJ, Suemoto Y, Meyerhardt JA, Fuchs CS. Molecular correlates with MGMT promoter methylation and silencing support CpG island methylator phenotype-low (CIMP-low) in colorectal cancer. Gut 2007; 56: 1564-1571.

[84**]** Attri J, Srinivasan R, Majumdar S, Radotra BD, Wig J. Alterations of tumor suppressor gene p16INK4a in pancreatic ductal carcinoma. BMC Gastroenterol. 2005; 5: 22.

[85] Mardin WA, Petrov KO, Enns A, Senninger N, Haier J, Mees ST. SERPINB5 and AKAP12 - expression and promoter methylation of metastasis suppressor genes in pancreatic ductal adenocarcinoma. BMC Cancer 2010; 10: 549.

[86] Cavallari I, Silic-Benussi M, Rende F, Martines A, Fogar P, Basso D, Vella MD, Pedrazzoli S, Herman JG, Chieco-Bianchi L, Esposito G, Ciminale V, D'Agostino DM. Decreased expression and promoter methylation of the menin tumor suppressor in pancreatic ductal adenocarcinoma. Genes Chromosomes Cancer 2009; 48: 383-396.

[87] Frommer M, McDonald LE, Millar DS, Collis CM, Watt F, Grigg GW, Molloy PL, Paul CL. A genomic sequencing protocol that yields a positive display of 5-

methylcytosine residues in individual DNA strands. Proc Natl Acad Sci USA 1992; 89: 1827–1831.

[88] Eulalio A, Huntzinger E, Izaurralde E. Getting to the root of miRNA-mediated gene silencing. Cell 2008; 132: 9-14.

[89] Aleman LM, Doench J, Sharp PA. Comparison of siRNA-induced off-target RNA and protein effects. RNA 2007; 13: 385-395.

[90] Schickel R, Boyerinas B, Park SM, Peter ME. MicroRNAs: key players in the immune system, differentiation, tumorigenesis and cell death. Oncogene 2008; 27: 5959-5974.

[91] Medina PP, Slack FJ. MicroRNAs and cancer: an overview. Cell Cycle 2008; 7: 2485-2492.

[92] Gironella M, Seux M, Xie MJ, Cano C, Tomasini R, Gommeaux J, Garcia S, Nowak J, Yeung ML, Jeang KT, Chaix A, Fazli L, Motoo Y, Wang Q, Rocchi P, Russo A, Gleave M, Dagorn JC, Iovanna JL, Carrier A, Pébusque MJ, Dusetti NJ. Tumor protein 53-induced nuclear protein 1 expression is repressed by miR-155, and its restoration inhibits pancreatic tumor development. Proc Natl Acad Sci U S A 2007; 104: 16170-16175.

[93] Bhatti I, Lee A, James V, Hall RI, Lund JN, Tufarelli C, Lobo DN, Larvin M. Knockdown of microRNA-21 inhibits proliferation and increases cell death by targeting programmed cell death 4 (PDCD4) in pancreatic ductal adenocarcinoma. J Gastrointest Surg 2011; 15: 199-208.

[94] Chen X, Ba Y, Ma L, Cai X, Yin Y, Wang K, Guo J, Zhang Y, Chen J, Guo X, Li Q, Li X, Wang W, Zhang Y, Wang J, Jiang X, Xiang Y, Xu C, Zheng P, Zhang J, Li

R, Zhang H, Shang X, Gong T, Ning G, Wang J, Zen K, Zhang J, Zhang CY. Characterization of microRNAs in serum: a novel class of biomarkers for diagnosis of cancer and other diseases. Cell Res 2008; 18: 997-1006.

[95] Weiler J, Hunziker J, Hall J. Anti-miRNA oligonucleotides (AMOs): ammunition to target miRNAs implicated in human disease? Gene Ther 2006; 13: 496-502.

[96] Wurdinger T, Costa FF. Molecular therapy in the microRNA era. Pharmacogenomics J 2007; 7: 297-304.

[97] Bloomston M, Frankel WL, Petrocca F, Volinia S, Alder H, Hagan JP, Liu CG, Bhatt D, Taccioli C, Croce CM. MicroRNA expression patterns to differentiate pancreatic adenocarcinoma from normal pancreas and chronic pancreatitis. JAMA 2007; 297: 1901-1908.

[98] Szafranska AE, Davison TS, John J, Cannon T, Sipos B, Maghnouj A, Labourier E, Hahn SA. MicroRNA expression alterations are linked to tumorigenesis and non-neoplastic processes in pancreatic ductal adenocarcinoma. Oncogene 2007; 26: 4442-4452.

[99] Lee EJ, Gusev Y, Jiang J, Nuovo GJ, Lerner MR, Frankel WL, Morgan DL, Postier RG, Brackett DJ, Schmittgen TD. Expression profiling identifies microRNA signature in pancreatic cancer. Int J Cancer 2007; 120: 1046-1054.

[100] Betel D, Wilson M, Gabow A, Marks DS, Sander C. The microRNA.org resource: targets and expression. Nucleic Acids Res 2008; 36: D149-153.

[101] Krutzfeldt J, Rajewsky N, Braich R, Rajeev KG, Tuschl T, Manoharan M, Stoffel M. Silencing of microrna in vivo with 'antagomirs'. Nature 2005; 438: 685-689.

[102] Available from: http://bioinformatics.mdanderson.org/Software/OOMPA/

[103] Ingenuity Pathways Analysis software web link, http://www.ingenuity.com/

[104] Lee KM, Nguyen C, Ulrich AB, Pour PM, Ouellette MM. Immortalization with telomerase of the Nestin-positive cells of the human pancreas. Biochem Biophys Res Commun 2003; 301: 1038-1044.

[105] Grimson A, Farh KK, Johnston WK, Garrett-Engele P, Lim LP, Bartel DP. MicroRNA targeting specificity in mammals: determinants beyond seed pairing. Mol Cell 2007; 27: 91-105.

[106] Krek A, Grun D, Poy MN, Wolf R, Rosenberg L, Epstein EJ, MacMenamin P, da Piedade I, Gunsalus KC, Stoffel M, Rajewsky N. Combinatorial microRNA target predictions. Nat Genet 2005; 37: 495-500.

[107] Velu CS, Baktula AM, Grimes HL. Gfi1 regulates miR-21 and miR-196b to control myelopoiesis. Blood 2009; 113: 4720-4728.

[108] Wu S, Huang S, Ding J, Zhao Y, Liang L, Liu T, Zhan R, He X. Multiple microRNAs modulate p21Cip1/Waf1 expression by directly targeting its 3' untranslated region. Oncogene 2010; 29: 2302-2308.

[109] Ding XC, Weiler J, Grosshans H. Regulating the regulators: mechanisms controlling the maturation of microRNAs. Trends Biotechnol 2009; 27: 27-36.

[110] Guo H, Ingolia NT, Weissman JS, Bartel DP. Mammalian microRNAs predominantly act to decrease target mRNA levels. Nature 2010; 466: 835-840.

[111] Greenbaum D, Colangelo C, Williams K, Gerstein M. Comparing protein abundance and mRNA expression levels on a genomic scale. Genome Biol 2003; 4: 117.

[112] Larsson E, Sander C, Marks D. mRNA turnover rate limits siRNA and microRNA efficacy. Mol Syst Biol 2010; 6: 433.

[113] Frazier ML, Pathak S, Wang ZW, Cleary K, Singletary SE, Olive M, Mackay B, Steck PA, Levin B. Establishment of a new human pancreatic adenocarcinoma cell line, MDAPanc-3. Pancreas 1990; 5: 8-16.

[114] Yunis AA, Arimura GK, Russin DJ. Human pancreatic carcinoma (MIA PaCa-2) in continuous culture: sensitivity to asparaginase. Int J Cancer 1977; 19: 128-135.

[115] Sirivatanauksorn V, Sirivatanauksorn Y, Gorman PA, Davidson JM, Sheer D, Moore PS, Scarpa A, Edwards PA, Lemoine NR. Non-random chromosomal rearrangements in pancreatic cancer cell lines identified by spectral karyotyping. Int J Cancer 2001; 91: 350-358.

[116] Tili E, Croce CM, Michaille JJ. miR-155: on the crosstalk between inflammation and cancer. Int Rev Immunol 2009; 28: 264-284.

[117] Faraoni I, Antonetti FR, Cardone J, Bonmassar E. miR-155 gene: a typical multifunctional microRNA. Biochim Biophys Acta 2009; 1792: 497-505.

[118] Wang J, Chen J, Chang P, LeBlanc A, Li D, Abbruzzesse JL, Frazier ML, Killary AM, Sen S. MicroRNAs in plasma of pancreatic ductal adenocarcinoma patients as novel blood based biomarkers of disease. Cancer Prev Res 2009; 2: 807-813.

[119] Habbe N, Koorstra JB, Mendell JT, Offerhaus GJ, Ryu JK, Feldmann G, Mullendore ME, Goggins MG, Hong SM, Maitra A. MicroRNA miR-155 is a biomarker of early pancreatic neoplasia. Cancer Biol Ther 2009; 8: 340-346.

[120] Knudson AG Jr. Mutation and cancer: statistical study of retinoblastoma. Proc Natl Acad Sci U S A 1971; 68: 820-823.

[121] Chai H, Brown RE. Field effect in cancer-an update. Ann Clin Lab Sci 2009; 39: 331-337.

[122] Strahl BD, Allis CD. The language of covalent histone modifications. Nature 2000; 403: 41-45.

[123] Jenuwein T, Allis CD. Translating the histone code. Science 2001; 293: 1074-1080.

[124] Tam OH, Aravin AA, Stein P, Girard A, Murchison EP, Cheloufi S, Hodges E, Anger M, Sachidanandam R, Schultz RM, Hannon GJ. Pseudogene-derived small interfering RNAs regulate gene expression in mouse oocytes. Nature 2008; 453: 534-538.

[125] Watanabe T, Totoki Y, Toyoda A, Kaneda M, Kuramochi-Miyagawa S, Obata Y, Chiba H, Kohara Y, Kono T, Nakano T, Surani MA, Sakaki Y, Sasaki H. Endogenous siRNAs from naturally formed dsRNAs regulate transcripts in mouse oocytes. Nature 2008; 453: 539-543.

[126] Poliseno, L, Salmena L, Zhang J, Carver B, Haveman WJ, Pandolfi PP. A coding-independent function of gene and pseudogene mRNAs regulates tumour biology. Nature 2010; 465: 1033-1038.

VITA

Qian Liu was born in Shenyang City, Liaoning Province, P. R. China on November 1st, 1973. As the only child of her family, she chose to go to China Medical University where her parents were working. She earned a M.D. degree after 6 years of study and became a Teaching and Research Assistant in the Department of Biochemistry in the same university. Two years later, she went to Kagawa Medical University in Japan as a Visiting Scientist for one year. At the end of year 2001, she followed her husband to Houston, Texas. Since then, she stayed in this city for almost 10 years. After more than 3 years working in the Department of Genetics in Baylor College of Medicine, Qian Liu decided to go back to school. Luckily, her application was accepted by the Graduate School of Biomedical Sciences, The University of Texas in Houston, and she started her Ph.D. study from 2005 fall semester. Now, she is a proud mom of two sons and will continue her career in Cancer Research.

Address:

2306 Shadow Falls Lane, Pearland, TX 77584